
A Neural Framework for Learning Subgraph and Graph Similarity Measures

| | |
|----------------------------------------------------------------------------------------------|-------------------------------------------------------------------------------|
| Rishabh Ranjan IIT Delhi, India rishabh.ranjan.cs118@cse.iitd.ac.in | Siddharth Grover IIT Delhi, India siddharth.grover11@gmail.com |
| Sourav Medya Northwestern University, USA sourav.medya@kellogg.northwestern.edu | Venkatesan Chakaravarthy IBM Research, India vechakra@in.ibm.com |
| Yogish Sabharwal IBM Research, India ysabharwal@in.ibm.com | Sayan Ranu IIT Delhi, India sayanranu@iitd.ac.in |

Abstract

Subgraph similarity search is a fundamental operator in graph analysis. In this framework, given a query graph and a graph database, the goal is to identify subgraphs of the database graphs that are structurally similar to the query. *Subgraph edit distance* (SED) is one of the most expressive measures for subgraph similarity. In this work, we study the problem of *learning* SED from a training set of graph pairs and their SED values. Towards that end, we design a novel *siamese* graph neural network called NEUROSED, which learns an embedding space with a rich structure reminiscent of SED. With the help of a specially crafted inductive bias, NEUROSED not only enables high accuracy but also ensures that the predicted SED, like true SED, satisfies *triangle inequality*. The design is generic enough to also model *graph edit distance* (GED), while ensuring that the predicted GED space is *metric*, like the true GED space. Extensive experiments on real graph datasets, for both SED and GED, establish that NEUROSED achieves ≈ 2 times lower RMSE than the state of the art and is ≈ 18 times faster than the fastest baseline. Further, owing to its pair-independent embeddings and theoretical properties, NEUROSED allows ≈ 3 orders of magnitude faster retrieval of graphs and subgraphs.

1 Introduction and Related work

Graphs are used to model data in a wide variety of domains. Examples include chemical compounds [44], protein-protein interaction networks (PPI) [1], knowledge graphs [17], and social networks [26]. A distance function on any dataset, including graphs, is a fundamental operator. Among several distance measures on graphs, *edit distance* is one of the most powerful and popular mechanisms [35, 54, 9, 14, 19, 42, 51, 22]. Edit distance can be posed in two forms: *graph edit distance* (GED) and *subgraph edit distance* (SED). Given two graphs \mathcal{G}_1 and \mathcal{G}_2 , $\text{GED}(\mathcal{G}_1, \mathcal{G}_2)$ returns the minimum cost of edits needed to convert \mathcal{G}_1 to \mathcal{G}_2 . i.e., for \mathcal{G}_1 to become *isomorphic* to \mathcal{G}_2 . An edit can be addition or deletion of edges and nodes, or replacement of edge or node labels, with an associated cost. In $\text{SED}(\mathcal{G}_1, \mathcal{G}_2)$, the goal is to identify the minimum cost of edits so that \mathcal{G}_1 is *subgraph isomorphic* to \mathcal{G}_2 . For examples, see Fig. 1a. We define these notions more formally in § 2.

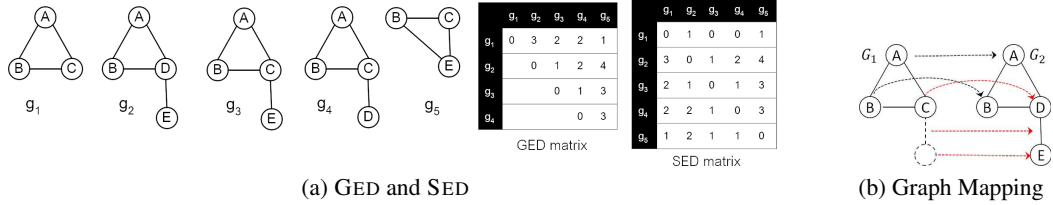


Figure 1: (a) A sample set of graphs and their corresponding GED and SED matrices. (b) Example of a graph mapping. The dashed nodes and edges represent dummy nodes and edges. The red arrows denote either insertion or change of label.

GED is typically restricted to graph databases containing small graphs to facilitate distance computation with queries of similar sizes. As an example, given a repository of molecules, and a query molecule, we may want to identify the closest molecule in the repository that is similar to the query. SED, on the other hand, is useful when the database has large graphs and the query is a comparatively smaller graph. As examples, subgraph queries are used on knowledge graphs for analogy reasoning [17]. In PPI and chemical compounds, SED is of central importance to identify functional motifs and binding pockets [44, 22, 16].

While the applications of GED and SED are beyond doubt, their applicability is constrained by their computation costs. Specifically, both GED and SED are NP-complete [51, 38, 22]. To mitigate this computational bottleneck, several heuristics [9, 14, 19, 42, 38] and index structures [22, 51, 35, 54] have been proposed. Recently, graph neural networks have been shown to be effective in learning and predicting GED [2, 47, 34, 3, 53, 48] and subgraph isomorphism [37]. The basic goal in all these algorithms is to learn a neural model from a training set of graph pairs and their distances, such that, at inference time, given an unseen graph pair, we are able to predict its distance accurately. While this progress in the area of graph querying is undoubtedly impressive, there is scope to do more.

- **Modeling SED:** Existing neural approaches to learning GED cannot easily be adapted to learn SED. While GED is symmetric, SED is not. Most neural architectures for GED have the assumption of symmetry at its core and hence modeling SED is non-trivial. In App. A, we provide a detailed analysis of the limitations of prior architectures in failing to model SED.
- **Exponential Search Space:** Computing $\text{SED}(\mathcal{G}_1, \mathcal{G}_2)$ conceptually requires us to compare the query graph \mathcal{G}_1 with the exponentially many subgraphs of the target graph \mathcal{G}_2 . Therefore, it is imperative that the model has an efficient and effective mechanism to prune the search space without compromising on the prediction accuracy. We note that while several index structures and heuristics exist for GED [22, 51, 2, 47], none exist for SED. Thus, scalability of SED on large graphs remains an unsolved problem.
- **Preservation of theoretical properties:** GED is a *metric* distance function. While SED is not metric due to being asymmetric, it satisfies *triangle inequality*, *non-negativity*, and *subgraph-identity*. Several higher-order tasks such as clustering and indexing rely on such properties [21, 15, 24, 43, 46, 50, 52, 10, 12]. Existing neural approaches do not preserve these properties, which limits their usability for these higher order tasks.
- **Pair-independent embedding:** There is little scope for pre-computation in existing approaches (either neural or non-neural), as the major computations are pair-dependent, i.e., both \mathcal{G}_1 and \mathcal{G}_2 need to be known. In a typical graph querying framework, the graph database is known apriori; only the query graph is provided at runtime. If we can generate *pair-independent* embeddings, and make efficient predictions directly in the embedding space, then retrieval can be sped up tremendously by pre-computing and indexing the embeddings of the database graphs beforehand.
- **Learning with low-volume data:** Generating a large amount of high quality training data is computationally prohibitive for SED/GED. So, an effective model should encode powerful priors for SED/GED prediction, to enable generalization even with scarce training data.

We address these challenges by a novel architecture called NEUROSED. Our key contributions are:

- **Novel formulation:** We formulate the problem of learning subgraph edit distance (SED) for graphs. Since SED is more general than subgraph isomorphism and GED, the proposed theory extends to prediction of GED, graph isomorphism and subgraph isomorphism.
- **Neural architecture:** NEUROSED utilizes a *siamese graph isomorphism network* [49] to embed graphs in a *pair-independent* fashion to an embedding space over which a simple function can predict the SED (or GED). The same embedding model is used for both \mathcal{G}_1 and \mathcal{G}_2 , which captures the prior that similar topological properties need to be considered for both graphs. The carefully crafted prediction function serves as another *inductive bias* for the model, which, in addition to enabling high generalisation accuracy, preserves the key properties of SED/GED, which is a major contribution of our work over existing neural approaches.
- **Indexable embeddings:** The prediction function satisfies triangle inequality over the embedding space for both SED and GED. This allows utilization of the rich literature on index structures [18, 30, 13] for boosting querying efficiency.
- **Accurate, Fast and Scalable:** Extensive experiments on real graph datasets containing up to a million nodes establish that NEUROSED is more accurate in both GED and SED when compared to the state of the art and is more than 3 orders of magnitude faster in range and k -NN queries.

2 Preliminaries and Problem Formulation

We denote a labelled undirected graph as $\mathcal{G} = (\mathcal{V}, \mathcal{E}, \mathcal{L})$ where \mathcal{V} is the node set, \mathcal{E} is the edge set and $\mathcal{L} : \mathcal{V} \cup \mathcal{E} \rightarrow \Sigma$ is the labeling function over nodes and edges. Σ is the universe of all labels and contains a special empty label ϵ . $\mathcal{L}(v)$ and $\mathcal{L}(e)$ denotes the labels of node v and edge e respectively. $\mathcal{G}_1 \subseteq \mathcal{G}_2$ denotes that \mathcal{G}_1 is a *subgraph* of \mathcal{G}_2 . For the definitions of *subgraph* and *graph isomorphism*, refer to App. B in the supplementary. The computation of GED relies on a *graph mapping*.

Definition 1 (Graph Mapping) *Given two graphs \mathcal{G}_1 and \mathcal{G}_2 , let $\tilde{\mathcal{G}}_1 = (\tilde{\mathcal{V}}_1, \tilde{\mathcal{E}}_1, \tilde{\mathcal{L}}_1)$ and $\tilde{\mathcal{G}}_2 = (\tilde{\mathcal{V}}_2, \tilde{\mathcal{E}}_2, \tilde{\mathcal{L}}_2)$ be obtained by adding dummy nodes and edges (labeled with ϵ) to \mathcal{G}_1 and \mathcal{G}_2 respectively, such that $|\mathcal{V}_1| = |\mathcal{V}_2|$ and $|\mathcal{E}_1| = |\mathcal{E}_2|$. A node mapping between \mathcal{G}_1 and \mathcal{G}_2 is a bijection $\pi : \tilde{\mathcal{G}}_1 \rightarrow \tilde{\mathcal{G}}_2$ where (i) $\forall v \in \tilde{\mathcal{V}}_1, \pi(v) \in \tilde{\mathcal{V}}_2$ and at least one of v and $\pi(v)$ is not a dummy; (ii) $\forall e = (v_1, v_2) \in \tilde{\mathcal{E}}_1, \pi(e) = (\pi(v_1), \pi(v_2)) \in \tilde{\mathcal{E}}_2$ and at least one of e and $\pi(e)$ is not a dummy.*

Example 1 Fig. 1b shows a graph mapping. Edge mappings can be trivially inferred, so are omitted.

Definition 2 (Graph Edit Distance (GED) under mapping π) GED between \mathcal{G}_1 and \mathcal{G}_2 under π is

$$\text{GED}_\pi(\mathcal{G}_1, \mathcal{G}_2) = \sum_{v \in \tilde{\mathcal{V}}_1} d(\mathcal{L}(v), \mathcal{L}(\pi(v))) + \sum_{e \in \tilde{\mathcal{E}}_1} d(\mathcal{L}(e), \mathcal{L}(\pi(e))) \quad (1)$$

where $d : \Sigma \times \Sigma \rightarrow \mathbb{R}_0^+$ is a distance function over the label set.

$d(\ell_1, \ell_2)$ models an *insertion* if $\ell_1 = \epsilon$, *deletion* if $\ell_2 = \epsilon$ and *replacement* if $\ell_1 \neq \ell_2$ and neither ℓ_1 nor ℓ_2 is a dummy. We assume d to be a binary function, where $d(\ell_1, \ell_2) = 1$ if $\ell_1 \neq \ell_2$, otherwise, 0. Our framework easily extends to more general distance functions (details in App. D).

Example 2 GED for the shown mapping in Fig. 1b is 3. The red mappings incur a cost of 1.

Definition 3 (Graph Edit Distance (GED)) GED is the minimum distance under all mappings.

$$\text{GED}(\mathcal{G}_1, \mathcal{G}_2) = \min_{\forall \pi \in \Phi(\mathcal{G}_1, \mathcal{G}_2)} \text{GED}_\pi(\mathcal{G}_1, \mathcal{G}_2) \quad (2)$$

where $\Phi(\mathcal{G}_1, \mathcal{G}_2)$ denotes the set of all possible node maps from \mathcal{G}_1 to \mathcal{G}_2 .

Definition 4 (Subgraph Edit Distance (SED)) SED is the minimum GED over all subgraphs of \mathcal{G}_2 .

$$\text{SED}(\mathcal{G}_1, \mathcal{G}_2) = \min_{\mathcal{S} \subseteq \mathcal{G}_2} \text{GED}(\mathcal{G}_1, \mathcal{S}) \quad (3)$$

Example 3 Revisiting Fig. 1b, $\text{GED}(\mathcal{G}_1, \mathcal{G}_2) = 3$. The shown mapping incurs the minimum cost. $\text{SED}(\mathcal{G}_1, \mathcal{G}_2) = 1$. Refer to Fig. 1a for more examples.

Problem 1 (Learning SED) Given a training set of tuples of the form $\langle \mathcal{G}_1, \mathcal{G}_2, \text{SED}(\mathcal{G}_1, \mathcal{G}_2) \rangle$, learn a neural model to predict $\text{SED}(\mathcal{Q}_1, \mathcal{Q}_2)$ on unseen graphs \mathcal{Q}_1 and \mathcal{Q}_2 .

Problem 2 (Learning GED) Given a training set of tuples of the form $\langle \mathcal{G}_1, \mathcal{G}_2, \text{GED}(\mathcal{G}_1, \mathcal{G}_2) \rangle$, learn a neural model to predict $\text{GED}(\mathcal{Q}_1, \mathcal{Q}_2)$ on unseen graphs \mathcal{Q}_1 and \mathcal{Q}_2 .

2.1 Properties of SED and GED

Observation 1 (i) $\text{GED}(\mathcal{G}_1, \mathcal{G}_2) \geq 0$, (ii) $\text{SED}(\mathcal{G}_1, \mathcal{G}_2) \geq 0$.

Observation 2 (i) $\text{GED}(\mathcal{G}_1, \mathcal{G}_2) = 0$ iff \mathcal{G}_1 is isomorphic to \mathcal{G}_2 , (ii) $\text{SED}(\mathcal{G}_1, \mathcal{G}_2) = 0$ iff \mathcal{G}_1 is subgraph isomorphic to \mathcal{G}_2 .

Observation 3 GED is a metric if the distance function d over label set Σ is metric [22]. d as defined in § 2 is metric [22]. Hence, GED from § 2 is metric.

We next prove that SED satisfies triangle inequality in Theorem 1.

Theorem 1 $\text{SED}(\mathcal{G}_1, \mathcal{G}_3) \leq \text{SED}(\mathcal{G}_1, \mathcal{G}_2) + \text{SED}(\mathcal{G}_2, \mathcal{G}_3)$.

PROOF SKETCH: Lemma 3 (App. D.1) shows that SED can be viewed as GED under a modified cost function. Specifically, the SED is equivalent to GED with a label set distance function where we ignore insertion costs. Furthermore, this modified distance function satisfies triangle inequality, which leads to triangle inequality for SED (similar to Observation 3). See App. D.1 for details. \square

3 NEUROSED

Fig. 2 presents the architecture of NEUROSED. The input to our learning framework is a pair of graphs \mathcal{G}_Q (query), \mathcal{G}_T (target) along with the supervision data $\text{SED}(\mathcal{G}_Q, \mathcal{G}_T)$. Our objective is to train a model that can predict SED on unseen query and target graphs. The design of our model must be cognizant of the fact that computing SED is NP-hard and high quality training data is scarce. Thus, we use a *Siamese* architecture in which the weight sharing between the embedding models boosts learnability and generalization from low-volume data by imposing a strong prior that the same topological features must be extracted for both graphs.

Siamese Networks: Siamese networks [11] are neural network models that were originally proposed for visual similarity learning, for which they have achieved significant success [29, 4]. In these models, there are *two* networks with *shared* parameters applied to two inputs independently to compute representations. These representations are then passed through another module to compute a similarity score.

3.1 Siamese Graph Neural Network

As depicted in Fig. 2a, we use a siamese graph neural network (GNN) with shared parameters to embed both \mathcal{G}_Q and \mathcal{G}_T . Fig. 2b focuses on the GNN component of NEUROSED. We next discuss each of its individual components.

Pre-MLP: The primary task of the Pre-MLP is to learn representations for the node labels (or features). Towards that end, let \mathbf{x}_v denote the initial feature set of node v . The MLP learns a hidden representation $\mu_v^G = \text{MLP}(\mathbf{x}_v)$. In our implementation, \mathbf{x}_v is a one-hot encoding of the categorical node labels. We do not explicitly model edge labels in our experiments. NEUROSED can easily be extended to edge labels, such as using GINE [25] layers instead of GIN layers (see App. C).

Graph Isomorphism Network (GIN): GIN [49] consumes the information from the Pre-MLP to learn hidden representations that encode both the graph structure as well as the node feature information. GIN is as powerful as the *Weisfeiler-Lehman (WL) graph isomorphism test* [31] in distinguishing graph structures. Since our goal is to accurately characterize graph topology and learn

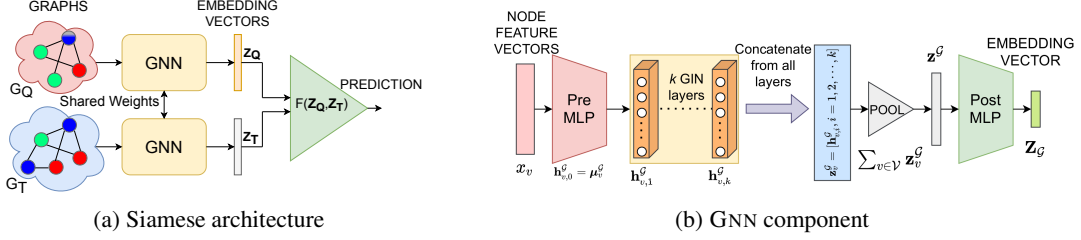


Figure 2: The architecture of NEUROSED.

similarity, GIN emerges as the natural choice. GIN develops its expressive power by using an *injective* aggregation function. Specifically, in the initial layer, each node v in graph \mathcal{G} is characterized by the representation learned by the MLP, i.e., $\mathbf{h}_{v,0}^G = \mu_v^G$. Subsequently, in each hidden layer i , we learn an embedding through the following transformation.

$$\mathbf{h}_{v,i}^G = \text{MLP} \left((1 + \epsilon^i) \cdot \mathbf{h}_{v,i-1}^G + \sum_{u \in \mathcal{N}_{\mathcal{G}}(v)} \mathbf{h}_{u,i-1}^G \right) \quad (4)$$

Here, ϵ^i is a layer-specific learnable parameter, $\mathcal{N}_{\mathcal{G}}(v)$ is one-hop neighbourhood of the node v , and $\mathbf{h}_{v,0}^G = \mu_v^G$. The k -th layer embedding is $\mathbf{h}_{v,k}^G$, where k is final hidden layer.

Concatenation, Pool and Post-MLP: Intuitively, $\mathbf{h}_{v,i}^G$ captures a feature-space representation of the i -hop neighborhood of v . Typically, GNNs operate on node or edge level predictive tasks, such as node classification or link prediction, and hence, the node representations are passed through an MLP for the final prediction task. In our problem, we need to capture a graph level representation. Furthermore, the representation should be rich enough to also capture the various subgraphs within the input graph so that SED can be predicted accurately. To fulfil these requirements, we first *concatenate* the representation of a node across *all* hidden layers, i.e., the final node embedding is $\mathbf{z}_v^G = \text{CONCAT}(\mathbf{h}_{v,i}^G, \forall i \in \{1, 2, \dots, k\})$. This allows us to capture a multi-granular view of the subgraphs centered on v at different radii in the range $[1, k]$. Next, to construct the graph-level representation, we perform a sum-pool, which adds the node representations to give a single vector. This information is then fed to the Post-MLP to enable post-processing. Mathematically:

$$\mathbf{Z}_G = \text{MLP}(\mathbf{z}_v^G) = \text{MLP} \left(\sum_{v \in \mathcal{V}} \mathbf{z}_v^G \right) \quad (5)$$

SED Prediction: The final task is to predict the SED as a function of query graph embedding \mathbf{Z}_{G_Q} and target graph embedding \mathbf{Z}_{G_T} . The natural choice would be to feed these embeddings into another MLP to learn $\text{SED}(\mathbf{Z}_{G_Q}, \mathbf{Z}_{G_T})$. This MLP can then be trained jointly with the graph embedding model in an *end-to-end* fashion. However, an MLP prediction does not have any theoretical guarantees.

To ensure preservation of original space properties, we introduce an *inductive bias* in the form of a simple fixed computation function $\mathcal{F}(\mathbf{Z}_{G_Q}, \mathbf{Z}_{G_T})$ to predict the SED. By training the model to produce embeddings \mathbf{Z}_{G_Q} and \mathbf{Z}_{G_T} such that $\mathcal{F}(\mathbf{Z}_{G_Q}, \mathbf{Z}_{G_T}) \approx \text{SED}(\mathbf{Z}_{G_Q}, \mathbf{Z}_{G_T})$, we enforce a rich structure on the embedding space. We show that these embeddings satisfy many key properties of the SED (and GED) function that existing neural algorithms fail to do [2, 47, 3, 53]. \mathcal{F} is defined as follows:

$$\mathcal{F}(\mathbf{Z}_{G_Q}, \mathbf{Z}_{G_T}) = \|\text{ReLU}(\mathbf{Z}_{G_Q} - \mathbf{Z}_{G_T})\|_2 = \|\max \{0, \mathbf{Z}_{G_Q} - \mathbf{Z}_{G_T}\}\|_2 \quad (6)$$

Intuitively, for those co-ordinates where the value of \mathbf{Z}_{G_Q} is greater than \mathbf{Z}_{G_T} ; a distance penalty is accounted by \mathcal{F} in terms of how much those values differ, otherwise \mathcal{F} considers 0. This follows the intuition that the SED accounts for those features of \mathcal{G}_Q that are not in \mathcal{G}_T . Moreover, consistent with SED, the additional features in \mathcal{G}_T that are not in \mathcal{G}_Q , do not incur any cost. Finally, the parameters

of the entire model are learned by minimizing the mean squared error¹ (here \mathbb{T} is the training set).

$$\mathcal{L} = \frac{1}{|\mathbb{T}|} \sum_{\forall (\mathcal{G}_Q, \mathcal{G}_T) \in \mathbb{T}} (\mathcal{F}(\mathbf{Z}_{\mathcal{G}_Q}, \mathbf{Z}_{\mathcal{G}_T}) - \text{SED}(\mathcal{G}_Q, \mathcal{G}_T))^2 \quad (7)$$

Adaptation for GED (NEUROSED_G): The architecture naturally extends to GED (denoted by NEUROSED_G) with a modification of the prediction function. Specifically, instead of Eq. 6, we use:

$$\mathcal{F}_g(\mathbf{Z}_{\mathcal{G}_Q}, \mathbf{Z}_{\mathcal{G}_T}) = \|\mathbf{Z}_{\mathcal{G}_Q} - \mathbf{Z}_{\mathcal{G}_T}\|_2 \quad (8)$$

3.2 Theoretical Characterization

Lemma 1 *The following properties hold on predicted SED $\mathcal{F}(\mathbf{Z}_{\mathcal{G}_Q}, \mathbf{Z}_{\mathcal{G}_T})$:*

1. $\mathcal{F}(\mathbf{Z}_{\mathcal{G}_Q}, \mathbf{Z}_{\mathcal{G}_T}) \geq 0$
2. $\mathcal{F}(\mathbf{Z}_{\mathcal{G}_Q}, \mathbf{Z}_{\mathcal{G}_T}) = 0 \iff \mathbf{Z}_{\mathcal{G}_Q} \leq \mathbf{Z}_{\mathcal{G}_T}$
3. $\mathcal{F}(\mathbf{Z}_{\mathcal{G}_Q}, \mathbf{Z}_{\mathcal{G}_T}) \leq \mathcal{F}(\mathbf{Z}_{\mathcal{G}_Q}, \mathbf{Z}_{\mathcal{G}'_T}) + \mathcal{F}(\mathbf{Z}_{\mathcal{G}'_T}, \mathbf{Z}_{\mathcal{G}_T})$

PROOF. Properties (1) and (2) follow from the definition of \mathcal{F} itself. Property (3) follows from the fact that we take the L_2 norm (holds for any monotonic norm, details are available in App. D). \square

We see that \mathcal{F} satisfies the analogue of properties of SED (§ 2.1). Conditions 1, 2, and 3 captures non-negativity, the subgraph relation [37], and triangle inequality respectively.

Lemma 2 *The predicted GED, i.e., \mathcal{F}_g is metric. (i) Non-negativity: $\mathcal{F}_g(\mathbf{Z}_{\mathcal{G}_Q}, \mathbf{Z}_{\mathcal{G}_T}) \geq 0$, (ii) Identity: $\mathcal{F}_g(\mathbf{Z}_{\mathcal{G}_Q}, \mathbf{Z}_{\mathcal{G}_T}) = 0 \iff \mathbf{Z}_{\mathcal{G}_Q} = \mathbf{Z}_{\mathcal{G}_T}$, (iii) Symmetry: $\mathcal{F}_g(\mathbf{Z}_{\mathcal{G}_Q}, \mathbf{Z}_{\mathcal{G}_T}) = \mathcal{F}_g(\mathbf{Z}_{\mathcal{G}_T}, \mathbf{Z}_{\mathcal{G}_Q})$, (iv) Triangle Inequality: $\mathcal{F}_g(\mathbf{Z}_{\mathcal{G}_Q}, \mathbf{Z}_{\mathcal{G}_T}) \leq \mathcal{F}_g(\mathbf{Z}_{\mathcal{G}_Q}, \mathbf{Z}_{\mathcal{G}'_T}) + \mathcal{F}_g(\mathbf{Z}_{\mathcal{G}'_T}, \mathbf{Z}_{\mathcal{G}_T})$.*

PROOF. Follows trivially from the fact that \mathcal{F}_g forms a Euclidean space. \square

Theorem 2 *The properties of SED (and GED) in § 2.1 are satisfied by the prediction functions NEUROSED_(G₁, G₂) (and the GED version NEUROSED_G(G₁, G₂)).*

PROOF SKETCH. (For SED) Let \mathcal{E} be the embedding function learned by NEUROSED’s GNN. Then $\text{NEUROSED}(\mathcal{G}_1, \mathcal{G}_2) = \mathcal{F}(\mathcal{E}(\mathcal{G}_1), \mathcal{E}(\mathcal{G}_2))$. Now, the relevant properties follow from Lemma 1. \square

We note here that if different embedding models were used for \mathcal{G}_1 and \mathcal{G}_2 , or if the embeddings were pair-dependent [34], then Theorem 2 would not hold.

Complexity analysis: Inference is *linear* in query and target sizes (see App. E for details).

4 Empirical Evaluation

In this section, we establish the following²:

- **Subgraph Search:** NEUROSED outperforms the state of the art approaches for SED prediction.
- **Graph Search:** NEUROSED_G, the variant to predict GED, outperforms the state of the art approaches for GED prediction.
- **Scalability:** NEUROSED and NEUROSED_G are orders of magnitude faster than existing approaches and scale well to graphs with millions of nodes.

4.1 Experimental Setup

Details on the hardware and software platform are provided in App. H.

¹Since SED computation is NP-hard, in App. F, we discuss a loss function based on SED lower and upper bounds, which are faster to compute.

²Code, data and experiments are available at <https://github.com/idea-iitd/NeuroSED>.

Datasets: Table 4.1 lists the datasets used for benchmarking. Further details on the dataset semantics are provided in the App. G. We include a mixture of both *graph databases* (#graphs >1), as well as *single large* graphs (#graphs = 1). Linux and IMDB contain unlabeled graphs.

| Name | Avg. $ \mathcal{V} $ | Avg. $ \mathcal{E} $ | $ \Sigma $ | #Graphs | $ \mathcal{V}_{\mathcal{Q}} $ | $ \mathcal{E}_{\mathcal{Q}} $ |
|----------|----------------------|----------------------|------------|---------|-------------------------------|-------------------------------|
| Dblp | 1.66M | 7.2M | 8 | 1 | 284 | 1692 |
| Amazon | 334k | 925k | 1 | 1 | 43 | 194 |
| PubMed | 19.7k | 44.3k | 3 | 1 | 12 | 11 |
| CiteSeer | 4.2k | 5.3k | 6 | 1 | 12 | 12 |
| Cora_ML | 3k | 8.2k | 7 | 1 | 11 | 11 |
| Protein | 38 | 70 | 3 | 1,071 | 9 | 11 |
| AIDS | 14 | 15 | 38 | 1,811 | 7 | 7 |
| AIDS' | 9 | 9 | 29 | 700 | 9 | 9 |
| Linux | 8 | 7 | 1 | 1,000 | 8 | 7 |
| IMDB | 13 | 65 | 1 | 1,500 | 13 | 65 |

Table 1: Datasets used for benchmarking.

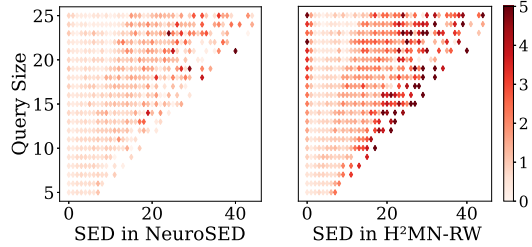


Figure 3: Heat Map of SED error against query size in DbLP. Darker means higher error.

Training (and Test) Data Generation: For GED, we use $\langle \text{query}, \text{target} \rangle$ graph pairs from IMDB, AIDS', and Linux. Our setup is identical to SIMGNN [2] and H²MN-RW [53]. For SED, the procedure is more intricate. The details of datasets can be found in App. G.

- **Targets:** For single large graphs, we generate target graphs from neighbourhoods (up to 5-hop) from every node in the graph. The average number of (nodes, edges) in target graphs from PubMed, CiteSeer, Cora_ML, Amazon and DbLP are (60, 129), (73, 192), (98, 179), (43, 97) and (240, 238) respectively. Theorem 3 in App. F justifies this neighborhood decomposition for subgraph search. For graph databases (Protein, AIDS', Linux and IMDB), each graph is a target.
- **Queries:** In single large graphs, queries are sampled by performing a random BFS traversal (depth upto 5) on a randomly chosen target graph. In addition, for AIDS, we use known *functional groups* from Table 1 in [41] as test queries. This allows us to benchmark NEUROSED on both natural as well synthetic queries. The average query sizes ($|\mathcal{V}_{\mathcal{Q}}|$, $|\mathcal{E}_{\mathcal{Q}}|$) are listed in Table 4.1.
- **Ground-truth:** We use *mixed integer programming* method F2 [32] implemented in GEDLIB [7] with a large time limit to generate ground-truth data.

Train-Validation-Test Split: We use 100K query-target pairs for training and 10K pairs each for validation and test. We also use data for 10 – 50 queries on all targets for ranking and range tests.

Baselines: To evaluate performance in **GED**, we compare with SIMGNN³ [2], GENN-A* [47] and H²MN[53]. H²MN has two versions based on random walks (H²MN-RW) and k -hop neighborhood (H²MN-NE). We include both.

For **SED**, no neural approaches exist. However, H²MN and SIMGNN can be trained by replacing GED with SED along with minor modifications in training. While NEUROMATCH [37] cannot predict SED, it generates a *violation score* which can be interpreted as the likelihood of the query being subgraph isomorphic to the target. The violation score can be used as a proxy for SED and used in ranking of k -NN (k -NearestNeighbour) queries. Thus, NEUROMATCH comparisons are limited to k -NN queries on SED. The changes required to adapt to SED are in App. H.

GNN [34] and GraphSim [3] are not included since they cannot be easily adapted for SED (See App. A for details). Furthermore, H²MN and GENN-A* are more recent, have better reported results, and therefore considered the state of the art. GENN-A* is not included for SED since it is exorbitantly slow and does not scale on graphs beyond 10 nodes (See Sec. 4.3).

In the **non-neural** category, we use *mixed integer programming* based method MIP-F2 [32] with a time bound of 0.1 seconds per pair for both GED and SED. MIP-F2 provides the optimal solution given infinite time. In addition, we also compare with BRANCH [5], which achieves an excellent trade-off between accuracy and runtime [6]. BRANCH uses *linear sum assignment problem with error-correction* (LSAPE) to process the search space. We use GEDLIB [7] for these methods.

³We use the PyTorch implementation of SIMGNN given on [paperswithcode](https://paperswithcode.com/sota/graph-edit-distance). The code of all other neural algorithms have been obtained from the respective authors.

| Methods | Dblp | Amazon | PubMed | CiteSeer | Cora_ML | Protein | AIDS | Methods | AIDS' | Linux | IMDB |
|----------------------|--------------|--------------|--------------|--------------|--------------|--------------|--------------|-----------------------|--------------|--------------|--------------|
| NEUROSED | 0.964 | 0.495 | 0.728 | 0.519 | 0.635 | 0.524 | 0.512 | NEUROSED _G | 0.796 | 0.415 | 6.734 |
| H ² MN-RW | 1.470 | 1.294 | 1.213 | 1.502 | 1.446 | 0.941 | 0.749 | H ² MN-RW | 0.994 | 0.734 | 86.077 |
| H ² MN-NE | 1.552 | 0.971 | 1.326 | 1.827 | 1.229 | 0.755 | 0.657 | H ² MN-NE | 1.000 | 0.319 | 87.594 |
| SIMGNN | 1.482 | 2.810 | 1.322 | 1.781 | 1.289 | 1.223 | 0.696 | GENN-A* | 0.907 | 0.267 | NA |
| Branch | 2.917 | 4.513 | 2.613 | 3.161 | 3.102 | 2.391 | 1.379 | SIMGNN | 1.037 | 0.666 | 66.250 |
| MIP-F2 | 3.427 | 5.595 | 3.399 | 4.474 | 3.871 | 2.249 | 1.537 | Branch | 3.322 | 2.474 | 6.875 |
| | | | | | | | | MIP-F2 | 2.929 | 1.245 | 82.124 |

(a) Prediction of SED.

(b) Prediction of GED

Table 2: **RMSE scores (lower is better) in (a) SED and (b) GED. GENN-A* does not scale on graphs beyond 10 nodes and hence the results in IMDB are not reported.**

4.2 Prediction Accuracy of SED and GED

Tables 2a and 2b present the accuracy of all techniques on SED and GED in terms of *Root Mean Square Error (RMSE)*. In App. I, we evaluate the same performance using several other metrics such as R^2 and Mean Absolute Error (MAE). NEUROSED outperforms all other techniques in 9 out of 10 settings. The gap in accuracy is the highest in IMDB for GED, where NEUROSED is more than 10 times better than the neural baselines. A deeper analysis reveals that IMDB graphs are significantly denser and larger than AIDS' or Linux. Thus, computing the optimal GED is harder. While all techniques have higher errors in IMDB, the deterioration is more severe in the baselines indicating that NEUROSED scales better with graph sizes.

To gain insight on whether the same patterns also hold in SED, in Fig. 3, we plot the *heat map* of RMSE against query graph size in Dblp. Specifically in this plot, each dot corresponds to a query graph \mathcal{G}_Q . The co-ordinate of a query is $(\text{SED}(\mathcal{G}_Q, \mathcal{G}_T), |\mathcal{V}_Q|)$. The color of a dot is the RMSE; the darker the color, the higher is the RMSE. When we compare the heat maps of NEUROSED with the most recent baseline H²MN-RW, we observe that H²MN-RW is noticeably darker. Furthermore, the dark colors are clustered on higher SED values and large query sizes (upper-right corner). This indicates that NEUROSED scales better with query size and higher SED. The heatmaps of all techniques for all datasets are provided in App. K.

Range and k-NN queries: Range and k -NN queries are two of the most common database queries. We next evaluate the performance of the various algorithms on these queries. In a range query, given a distance threshold θ , the goal is to retrieve all database graphs that are within θ distance from the query graph. In a k -NN query, given the query graph, we identify the k nearest neighbors from the search space in distance-ascending order. For SED, the search space includes all target graphs of the database graphs, whereas for GED, the search space constitutes of the database graphs. The performance measures are:

- **F1-score (Range query):** The accuracy is quantified using F1-score by comparing with the ground truth answer set.
- **Kendall's tau (k -NN) [27]:** κ measures how well the ranking is preserved between two ranked lists. In this case, we compare the ground truth rank order with the predicted.

As visible in Figs. 7a-7h, NEUROSED consistently outperforms all baselines in F1-score. Similar trend is also visible in k -NN queries. Specifically, in Kendall's tau (Tables 3a and 3b), barring the exception of GED in Linux, NEUROSED consistently scores the highest indicating best preservation of the ranking order. Overall, this shows that accurate prediction of distance also transfers to accurate querying accuracy. In App. I.2, we also report k -NN performance based on Precision@ k . In this analysis, we do not include GENN-A* since it is orders of magnitude slower than all neural-baselines and provides a comparable distance accuracy to H²MN. Next, we discuss efficiency in detail.

4.3 Efficiency

Table 4 presents the inference time per 10K graph pairs. As visible, NEUROSED is up to 1800 times faster than the non-neural baselines and up to 10 to 20 times faster than H²MN-RW, the current state of the art in GED prediction. Also note that GENN-A* is exorbitantly slow (Table 4b). GENN-A* is slower since it not only predicts the GED but also the alignment via an A* search. While the

| Methods | PubMed | CiteSeer | Cora_ML | Protein | AIDS |
|-------------|-------------|-------------|-------------|-------------|-------------|
| NEUROSED | 0.90 | 0.90 | 0.91 | 0.75 | 0.80 |
| H^2MN -RW | 0.87 | 0.88 | 0.88 | 0.70 | 0.72 |
| H^2MN -NE | 0.87 | 0.87 | 0.87 | 0.72 | 0.73 |
| SIMGNN | 0.85 | 0.87 | 0.86 | 0.63 | 0.73 |
| NEUROMATCH | 0.70 | 0.75 | 0.73 | 0.57 | 0.59 |

(a) Ranking in SED.

| Methods | AIDS' | Linux | IMDB |
|-----------------------|-------------|-------------|-------------|
| NEUROSED _G | 0.78 | 0.90 | 0.87 |
| H^2MN -RW | 0.72 | 0.89 | 0.80 |
| H^2MN -NE | 0.73 | 0.93 | 0.82 |
| SIMGNN | 0.70 | 0.84 | 0.70 |

(b) Ranking in GED

Table 3: Kendall's tau scores (higher is better).

| Methods | Dblp | Amazon | PubMed | CiteSeer | Cora_ML | Protein | AIDS |
|-------------|-------------|-------------|-------------|-------------|-------------|-------------|-------------|
| NEUROSED | 6.84 | 1.46 | 1.30 | 1.28 | 1.25 | 0.86 | 0.84 |
| H^2MN -RW | 44.68 | 23.2 | 25.79 | 27.54 | 29.04 | 19.33 | 9.63 |
| H^2MN -NE | 56.82 | 40.34 | 50.64 | 54.46 | 70.59 | 28.99 | 15.76 |
| SIMGNN | 109.56 | 47.68 | 39.80 | 39.40 | 40.73 | 39.02 | 43.83 |
| BRANCH | 626.489 | 79.25 | 99.11 | 155.09 | 132.98 | 52.26 | 12.93 |
| MIP-F2 | 1979.185 | 861.95 | 606.01 | 827.65 | 790.01 | 881.77 | 360.12 |

(a) SED.

| Methods | AIDS' | Linux | IMDB |
|-----------------------|-------------|-------------|-------------|
| NEUROSED _G | 0.49 | 0.70 | 0.63 |
| H^2MN -RW | 9.50 | 8.74 | 8.83 |
| H^2MN -NE | 10.38 | 9.80 | 10.69 |
| GENN-A* | 12190 | 1340 | NA |
| SIMGNN | 39.21 | 38.62 | 38.98 |
| BRANCH | 10.70 | 8.24 | 127.90 |
| MIP-F2 | 593.34 | 191.88 | 1173.548 |

(b) GED

Table 4: Running times of all methods in seconds per 10k pair (lower is better).

alignment information is indeed useful, computing this information across all graphs in the database may generate redundant information since an user is typically interested only on a small minority of graphs that are in the answer set. In App. I.4, we discuss this issue in detail.

Scalability: Here, we showcase how pair-independent embeddings, and ensuring triangle inequality leads to further boost in scalability. For this experiment, we use the three largest datasets of PubMed, Amazon and Dblp. For each dataset, we pre-compute NEUROSED embeddings of all database graphs by exploiting pair-independent embeddings. Such pre-computation is not possible in the neural or non-neural baselines. Furthermore, since the predictions of NEUROSED satisfy triangle inequality, we index the pre-computed embeddings of the database graphs using the Metric Tree [46] index structure adapted to asymmetric distance functions (see App. J). Consequently, for NEUROSED, we only need to embed the query graph and evaluate \mathcal{F} to make predictions at query time. Table 5 presents the results on range and 10-NN queries. When computations are done on a GPU, NEUROSED is more than 1000 times faster than both H^2MN -RW and H^2MN -NE. In the absence of a GPU, H^2MN is practically infeasible since expensive pair-dependent computations are done at query time. In contrast, even on a CPU, with tree indexing, NEUROSED is ≈ 50 times faster than GPU-based H^2MN . Note that indexing enables up to 3-times speed-up on NEUROSED over linear scan, which demonstrates the gain from ensuring triangle inequality. Overall, these results show the benefits of using an easily computable and parallelisable prediction function \mathcal{F} with theoretical guarantees.

4.4 Ablation Study

In this study, we explore the impact of our inductive biases in learning from low-volume data. We create two variants of NEUROSED: (1) NEUROSED-Dual trains the two parallel GNN models separately without weight-sharing, and (2) NEUROSED-NN uses an MLP instead of \mathcal{F} . Both have strictly higher representational capacity than NEUROSED. Figs. 5a-5c present the results. The RMSE of NEUROSED is consistently better than NEUROSED-Dual, with the difference being more significant at low volumes. This indicates that siamese structure helps. Compared to NEUROSED, NEUROSED-

| Datasets | Range ($\theta = 2$) | | | | | | 10-NN | | | | | |
|----------|------------------------|--------|--------|-------------|-------------|--------|--------|--------|-------------|-------------|--|--|
| | CPU | | GPU | | | | CPU | | GPU | | | |
| | L-Scan | M-Tree | L-Scan | H^2MN -RW | H^2MN -NE | L-Scan | M-Tree | L-Scan | H^2MN -RW | H^2MN -NE | | |
| Dblp | 48 | 20.9 | 0.070 | 696 | 8910 | 50.4 | 18.6 | 0.126 | 698 | 9790 | | |
| Amazon | 9.09 | 5.07 | 0.025 | 371 | 8550 | 11.3 | 4.75 | 0.027 | 372 | 8760 | | |
| PubMed | 0.693 | 0.56 | 0.004 | 26.6 | 35.2 | 1.01 | 0.49 | 0.004 | 27.5 | 35.5 | | |

Table 5: Querying time (s) for SED in the three largest datasets. L-Scan indicates time taken by linear scan in NEUROSED (times differs based on whether executed on a CPU or in GPU). M-Tree indicates time taken by NEUROSED when indexed using an adapted Metric Tree.

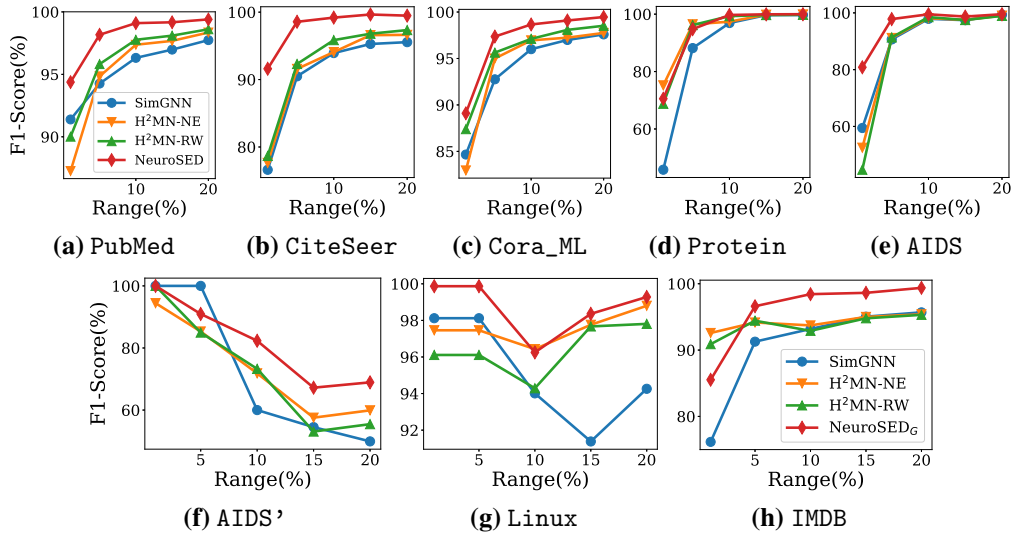


Figure 4: **F1-score in range queries on SED (a-e) and GED (f-h).** The range threshold is set as a percentage of the max distance observed in the test set.

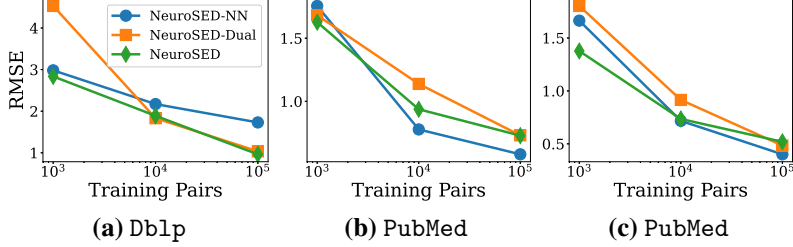


Figure 5: **Ablation study to analyze the impact of siamese architecture and function \mathcal{F} .**

NN achieves marginally better performance at larger train sizes in PubMed and CiteSeer. However, in Dblp, NEUROSED is consistently better. The number of subgraphs in a dataset grows exponentially with the node set size. Hence, an MLP needs growing training data to accurately model the intricacies of this search space. In Dblp, even 100k pairs is not enough to improve upon \mathcal{F} . Overall, these trends indicate that \mathcal{F} enables better generalization and scalability with respect to accuracy. Furthermore, given that its performance is close to an MLP, and it enables indexing, the benefits outweigh the marginal reduction in accuracy. More ablations studies are provided in App. I.3.

4.5 Visualization and Application of SED

Searching for molecular fragment containment is a routine task in drug discovery [40]. Motivated by this, we show the top-5 matches to an SED query on the AIDS dataset produced by NEUROSED in Fig. 6. The query is a functional group (Hydrogen atoms are not represented). NEUROSED is able to extract chemical compounds that contain this molecular fragment (except for ranks 3 and 5, which contain this group with 1 edit) from around 2000 chemical compounds with varying sizes and structures. This validates the efficacy of NEUROSED at a semantic level.

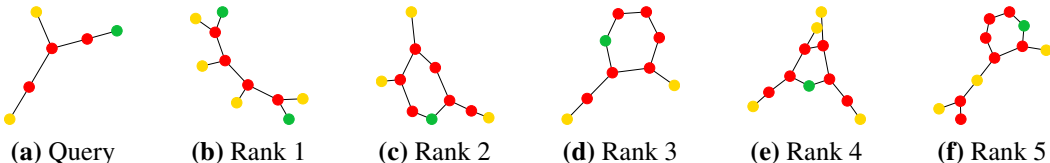


Figure 6: **Visualizations of query and resulting matches produced by NEUROSED.** Red, Green and Yellow colors indicate Carbon, Nitrogen and Oxygen atoms respectively. The actual and predicted SED for the target graphs are (b) 0, 0.4, (c) 0, 0.5, (d) 1, 0.6, (e) 0, 0.6 and (f) 1, 0.6.

5 Conclusions

Subgraph similarity search is a fundamental operator for graph analytics. Subgraph edit distance is one of the most popular similarity measures defined for subgraphs. The applicability of SED, however, is constrained by its exponential computation complexity. Our work is motivated by the following question: *Is it possible to design a neural framework that generalizes to both SED and GED, preserves their key properties and is capable of learning from a low-volume training data?* We show that this is indeed possible. The efficacy and efficiency of NEUROSED stems from three algorithmic innovations: a *siamese* architecture to reduce dependence on high-volume training data, a carefully designed function to introduce an inductive bias and mimic important properties of the original space, and pair-independent embeddings to enable massive scalability.

References

- [1] Noga Alon, Phuong Dao, Iman Hajirasouliha, Fereydoun Hormozdiari, and Süleyman Cenk Sahinalp. Biomolecular network motif counting and discovery by color coding. In *Proceedings 16th International Conference on Intelligent Systems for Molecular Biology (ISMB)*, pages 241–249, 2008.
- [2] Yunsheng Bai, Hao Ding, Song Bian, Ting Chen, Yizhou Sun, and Wei Wang. Simgnn: A neural network approach to fast graph similarity computation. In *Proceedings of the Twelfth ACM International Conference on Web Search and Data Mining*, WSDM ’19, page 384–392, 2019.
- [3] Yunsheng Bai, Hao Ding, Ken Gu, Yizhou Sun, and Wei Wang. Learning-based efficient graph similarity computation via multi-scale convolutional set matching. *Proceedings of the AAAI Conference on Artificial Intelligence*, 34(04):3219–3226, Apr. 2020.
- [4] Luca Bertinetto, Jack Valmadre, Joao F Henriques, Andrea Vedaldi, and Philip HS Torr. Fully-convolutional siamese networks for object tracking. In *European conference on computer vision*, pages 850–865. Springer, 2016.
- [5] David B Blumenthal. New techniques for graph edit distance computation. *arXiv preprint arXiv:1908.00265*, 2019.
- [6] David B Blumenthal, Nicolas Boria, Johann Gamper, Sébastien Bougleux, and Luc Brun. Comparing heuristics for graph edit distance computation. *The VLDB Journal*, 29(1):419–458, 2020.
- [7] David B Blumenthal, Sébastien Bougleux, Johann Gamper, and Luc Brun. Gedlib: a c++ library for graph edit distance computation. In *International Workshop on Graph-Based Representations in Pattern Recognition*, pages 14–24. Springer, 2019.
- [8] Aleksandar Bojchevski and Stephan Günnemann. Deep gaussian embedding of graphs: Unsupervised inductive learning via ranking. *arXiv preprint arXiv:1707.03815*, 2017.
- [9] Sébastien Bougleux, Luc Brun, Vincenzo Carletti, Pasquale Foggia, Benoit Gaüzère, and Mario Vento. Graph edit distance as a quadratic assignment problem. *Pattern Recognition Letters*, 87:38–46, 2017. Advances in Graph-based Pattern Recognition.
- [10] Sergey Brin. Near neighbor search in large metric spaces. In *Proceedings of the 21th International Conference on Very Large Data Bases*, VLDB ’95, page 574–584, San Francisco, CA, USA, 1995. Morgan Kaufmann Publishers Inc.
- [11] Jane Bromley, Isabelle Guyon, Yann LeCun, Eduard Säckinger, and Roopak Shah. Signature verification using a " siamese" time delay neural network. *Advances in neural information processing systems*, 6:737–744, 1993.
- [12] Edgar Chávez, Gonzalo Navarro, Ricardo Baeza-Yates, and Jose Marroquin. Searching in metric spaces. *ACM Comput. Surv.*, 33:273–321, 09 2001.
- [13] Paolo Ciaccia, Marco Patella, and Pavel Zezula. M-tree: An efficient access method for similarity search in metric spaces. In *VLDB*, 1997.
- [14] Évariste Daller, Sébastien Bougleux, Benoit Gaüzère, and Luc Brun. Approximate Graph Edit Distance by Several Local Searches in Parallel. In *7th International Conference on Pattern Recognition Applications and Methods*, 2018.

[15] Vlastislav Dohnal, Claudio Gennaro, Pasquale Savino, and Pavel Zezula. D-index: Distance searching index for metric data sets. *Multim. Tools Appl.*, 21(1):9–33, 2003.

[16] Chi Thang Duong, Trung Dung Hoang, Hongzhi Yin, Matthias Weidlich, Quoc Viet Hung Nguyen, and Karl Aberer. Efficient streaming subgraph isomorphism with graph neural networks. *Proc. VLDB Endow.*, 14(5):730–742, January 2021.

[17] Christopher L. Ebsch, Joseph A. Cottam, Natalie C. Heller, Rahul D. Deshmukh, and George Chin. Using graph edit distance for noisy subgraph matching of semantic property graphs. In *2020 IEEE International Conference on Big Data (Big Data)*, pages 2520–2525, 2020.

[18] Charles Elkan. Using the triangle inequality to accelerate k-means. In *Proceedings of the Twentieth International Conference on International Conference on Machine Learning*, ICML’03, page 147–153, 2003.

[19] Stefan Fankhauser, Kaspar Riesen, and Horst Bunke. Speeding up graph edit distance computation through fast bipartite matching. In *Proceedings of the 8th International Conference on Graph-Based Representations in Pattern Recognition*, page 102–111, 2011.

[20] Matthias Fey and Jan Eric Lenssen. Fast graph representation learning with pytorch geometric. *arXiv preprint arXiv:1903.02428*, 2019.

[21] Ali S. Hadi. Finding groups in data: An introduction to chster analysis. *Technometrics*, 34:111–112, 1991.

[22] Huahai He and Ambuj K Singh. Closure-tree: An index structure for graph queries. In *22nd International Conference on Data Engineering (ICDE)*, pages 38–38. IEEE, 2006.

[23] Kaiming He, Xiangyu Zhang, Shaoqing Ren, and Jian Sun. Deep residual learning for image recognition. In *Proceedings of the IEEE conference on computer vision and pattern recognition*, pages 770–778, 2016.

[24] Gisli R. Hjaltason and Hanan Samet. Index-driven similarity search in metric spaces (survey article). *ACM Trans. Database Syst.*, 28(4):517–580, December 2003.

[25] Weihua Hu, Bowen Liu, Joseph Gomes, Marinka Zitnik, Percy Liang, Vijay Pande, and Jure Leskovec. Strategies for pre-training graph neural networks. *arXiv preprint arXiv:1905.12265*, 2019.

[26] David Kempe, Jon Kleinberg, and Éva Tardos. Maximizing the spread of influence through a social network. In *Proceedings of the Ninth ACM SIGKDD International Conference on Knowledge Discovery and Data Mining*, page 137–146, 2003.

[27] M. G. Kendall. A new measure of rank correlation. *Biometrika*, 30(1/2):81–93, 1938.

[28] Thomas Kluyver, Benjamin Ragan-Kelley, Fernando Pérez, Brian E Granger, Matthias Bussonnier, Jonathan Frederic, Kyle Kelley, Jessica B Hamrick, Jason Grout, Sylvain Corlay, et al. Jupyter notebooks-a publishing format for reproducible computational workflows. In *International Conference on Electronic Publishing*, 2016.

[29] Gregory Koch, Richard Zemel, and Ruslan Salakhutdinov. Siamese neural networks for one-shot image recognition. In *ICML deep learning workshop*, volume 2. Lille, 2015.

[30] Wojciech Kwedlo and Paweł J. Czochanski. A hybrid mpi/openmp parallelization of \$k\\$-means algorithms accelerated using the triangle inequality. *IEEE Access*, 7:42280–42297, 2019.

[31] AA Leman and B Weisfeiler. A reduction of a graph to a canonical form and an algebra arising during this reduction. *Nauchno-Technicheskaya Informatsiya*, 2(9):12–16, 1968.

[32] Julien Lerouge, Zeina Abu-Aisheh, Romain Raveaux, Pierre Héroux, and Sébastien Adam. New binary linear programming formulation to compute the graph edit distance. *Pattern Recognition*, 72:254–265, 2017.

[33] Jure Leskovec and Rok Sosić. Snap: A general-purpose network analysis and graph-mining library. *ACM Transactions on Intelligent Systems and Technology (TIST)*, 8(1):1, 2016.

[34] Yujia Li, Chenjie Gu, Thomas Dullien, Oriol Vinyals, and Pushmeet Kohli. Graph matching networks for learning the similarity of graph structured objects. In *Proceedings of the 36th International Conference on Machine Learning*, pages 3835–3845, 2019.

[35] Yongjiang Liang and Peixiang Zhao. Similarity search in graph databases: A multi-layered indexing approach. In *2017 IEEE 33rd International Conference on Data Engineering (ICDE)*, pages 783–794, 2017.

[36] Ilya Loshchilov and Frank Hutter. Decoupled weight decay regularization. *arXiv preprint arXiv:1711.05101*, 2017.

[37] Zhaoyu Lou, Jiaxuan You, Chengtao Wen, Arquimedes Canedo, Jure Leskovec, et al. Neural subgraph matching. *arXiv preprint arXiv:2007.03092*, 2020.

[38] Michel Neuhaus, Kaspar Riesen, and Horst Bunke. Fast suboptimal algorithms for the computation of graph edit distance. In Dit-Yan Yeung, James T. Kwok, Ana Fred, Fabio Roli, and Dick de Ridder, editors, *Structural, Syntactic, and Statistical Pattern Recognition*, pages 163–172, Berlin, Heidelberg, 2006. Springer Berlin Heidelberg.

[39] Adam Paszke, Sam Gross, Francisco Massa, Adam Lerer, James Bradbury, Gregory Chanan, Trevor Killeen, Zeming Lin, Natalia Gimelshein, Luca Antiga, et al. Pytorch: An imperative style, high-performance deep learning library. *Advances in neural information processing systems*, 32:8026–8037, 2019.

[40] Sayan Ranu, Bradley T Calhoun, Ambuj K Singh, and S Joshua Swamidass. Probabilistic substructure mining from small-molecule screens. *Molecular Informatics*, 30(9):809–815, 2011.

[41] Sayan Ranu and Ambuj K Singh. Mining statistically significant molecular substructures for efficient molecular classification. *Journal of chemical information and modeling*, 49(11):2537–2550, 2009.

[42] Kaspar Riesen and Horst Bunke. Approximate graph edit distance computation by means of bipartite graph matching. *Image Vision Comput.*, 27(7):950–959, June 2009.

[43] Hanan Samet. *Foundations of Multidimensional and Metric Data Structures (The Morgan Kaufmann Series in Computer Graphics and Geometric Modeling)*. Morgan Kaufmann Publishers Inc., San Francisco, CA, USA, 2005.

[44] Aravind Sankar, Sayan Ranu, and Karthik Raman. Predicting novel metabolic pathways through subgraph mining. *Bioinformatics*, 33(24):3955–3963, 2017.

[45] Leslie N Smith. Cyclical learning rates for training neural networks. In *2017 IEEE winter conference on applications of computer vision (WACV)*, pages 464–472. IEEE, 2017.

[46] Jeffrey K. Uhlmann. Satisfying general proximity/similarity queries with metric trees. *Inf. Process. Lett.*, 40:175–179, 1991.

[47] Runzhong Wang, Tianqi Zhang, Tianshu Yu, Junchi Yan, and Xiaokang Yang. Combinatorial learning of graph edit distance via dynamic embedding. In *IEEE Conference on Computer Vision and Pattern Recognition, CVPR 2021, virtual, June 19-25, 2021*, pages 5241–5250, 2021.

[48] Haibo Xiu, Xiao Yan, Xiaoqiang Wang, James Cheng, and Lei Cao. Hierarchical graph matching network for graph similarity computation, 2020.

[49] Keyulu Xu, Weihua Hu, Jure Leskovec, and Stefanie Jegelka. How powerful are graph neural networks? *arXiv preprint arXiv:1810.00826*, 2018.

[50] Peter N. Yianilos. Data structures and algorithms for nearest neighbor search in general metric spaces. In *Proceedings of the Fourth Annual ACM-SIAM Symposium on Discrete Algorithms, SODA '93*, page 311–321, USA, 1993. Society for Industrial and Applied Mathematics.

[51] Zhiping Zeng, Anthony K. H. Tung, Jianyong Wang, Jianhua Feng, and Lizhu Zhou. Comparing stars: On approximating graph edit distance. *Proc. VLDB Endow.*, 2(1):25–36, August 2009.

[52] Pavel Zezula, Giuseppe Amato, Vlastislav Dohnal, and Michal Batko. *Similarity Search: The Metric Space Approach*, volume 32 of *Advances in Database Systems*. Springer, 2006.

[53] Zhen Zhang, Jiajun Bu, Martin Ester, Zhao Li, Chengwei Yao, Zhi Yu, and Can Wang. H2mn: Graph similarity learning with hierarchical hypergraph matching networks. In *KDD*, page 2274–2284, 2021.

[54] Xiang Zhao, Chuan Xiao, Xuemin Lin, Qing Liu, and Wenjie Zhang. A partition-based approach to structure similarity search. *Proc. VLDB Endow.*, 7(3):169–180, November 2013.

Appendix

A Inability of existing neural approaches GED in modeling SED

A key difference between SED and GED is that while GED is symmetric, SED is not. Hence, if the architecture or training procedure relies heavily on the assumption of symmetry, then the modeling capacity is compromised.

- **GMN [34]:** The loss function of GMN computes the euclidean distance between the embeddings and then this signal is used to learn the weight parameters (See Eq. 12 in [34]). The assumption of euclidean distance prohibits the model from learning an asymmetric distance function. Certainly, the loss function can be changed to incorporate an asymmetric distance measure and the performance of the architecture following this change may be studied. However, the selection of an appropriate loss function that works well with the GMN architecture is a research problem in itself. Apart from the loss function, the proposed architecture along with the attention mechanism is also motivated by symmetry (note the quantifications for i and j in Eqns. (4-8) in [34]).
- **GraphSim [3]:** GraphSim computes a square similarity matrix across node pairs of two graphs $\mathcal{G}_1 = (\mathcal{V}_1, \mathcal{E}_1)$, $\mathcal{G}_2 = (\mathcal{V}_2, \mathcal{E}_2)$ on which CNNs are applied to predict the similarity. Since \mathcal{G}_1 and \mathcal{G}_2 may be of different sizes, the smaller graph is padded with $||\mathcal{V}_1| - |\mathcal{V}_2||$ zeros. When the similarity matrix has a large number of zeros, it confuses the model into thinking that the two graphs are dissimilar. The authors of GraphSim acknowledge this themselves while justifying a padding of $||\mathcal{V}_1| - |\mathcal{V}_2||$ zeros instead of a fixed maximum size limit. We quote an exact line from the paper:
“the similarity matrix between two small but isomorphic graphs may be padded with a lot of zeros, potentially misleading the CNNs to predict they are dissimilar.”
In our problem, even if the query graph is significantly smaller than the target graph (tens of nodes vs. hundreds), SED can be 0. Thus, the above mentioned design of relying on node-to-node square similarity matrix is not well suited.
- **SimGNN [2]:** SimGNN relies on a neural tensor network and a pairwise node comparison module to compute similarity between two graphs. The pairwise node comparison module assumes the comparison matrix to be symmetric. Hence, in our adaptation of SimGNN for SED, we remove this particular module and only use the neural tensor network.

B Definitions

Definition 5 (Graph Isomorphism) Graph $\mathcal{G}_1 = (\mathcal{V}_1, \mathcal{E}_1, \mathcal{L}_1)$ is isomorphic to $\mathcal{G}_2 = (\mathcal{V}_2, \mathcal{E}_2, \mathcal{L}_2)$ if there exists a bijection $\pi : \mathcal{V}_1 \rightarrow \mathcal{V}_2$ such that (i) $\forall v \in \mathcal{V}_1 : \mathcal{L}(v) = \mathcal{L}(\pi(v))$, (ii) $\forall e = (v_1, v_2) \in \mathcal{E}_1 : \pi(e) = (\pi(v_1), \pi(v_2)) \in \mathcal{E}_2$, and (iii) $\forall e \in \mathcal{E}_1 : \mathcal{L}(e) = \mathcal{L}(\pi(e))$.

Subgraph isomorphism is defined analogously by using an *injection* instead of a bijection.

Definition 6 (Closest Subgraph) \mathcal{S} is a closest subgraph to \mathcal{G}_1 in \mathcal{G}_2 if $\text{SED}(\mathcal{G}_1, \mathcal{S}) = \text{GED}(\mathcal{G}_1, \mathcal{S})$.

C Handling Edge Labels

A straight-forward extension of NEUROSED to handle edge labels is to use GINE [25] layers instead of GIN layers. Equation 4 can be modified as follows:

$$\mathbf{h}_{v,i}^{\mathcal{G}} = \text{MLP} \left((1 + \epsilon^i) \cdot \mathbf{h}_{v,i-1}^{\mathcal{G}} + \sum_{u \in \mathcal{N}_{\mathcal{G}}(v)} \text{ReLU}(\mathbf{h}_{u,i-1}^{\mathcal{G}} + \mathbf{e}_{v,u}^{\mathcal{G}}) \right) \quad (9)$$

where $\mathbf{e}_{v,u}^{\mathcal{G}}$ denotes the vector representation of the edge label for edge (v, u) .

It is also possible to represent edge labels in the current architecture by constructing a new graph \mathcal{G}' with a vertex $w_{v,u}$ for every edge (v, u) and edges from v to $w_{v,u}$ and from $w_{v,u}$ to u . The node representation for $w_{v,u}$ is a vector representation for the label on the edge (v, u) (suitably padded

for uniformity). Furthermore a new dimension is introduced which separates these new nodes from the old ones and this dimension is set to 1 if the node is $w_{v,u}$ for some $(v, u) \in \mathcal{E}_G$ and 0 otherwise. NEUROSED (and NEUROSED $_{\mathcal{G}}$) can then be trained with such modified graphs as inputs, but using the ground truth SED (respectively GED) for the original graphs in the loss function.

D Additional Proofs

D.1 Triangle Inequality of SED: Proof of Theorem. 1

Our proof relies on two lemmas.

Lemma 3 *Let $\widehat{d} : \Sigma \times \Sigma \rightarrow \mathbb{R}_0^+$ be a distance function over Σ , where (i) $\widehat{d}(\ell_1, \ell_2) = 0$ if $\ell_1 = \ell_2$, and (ii) $\widehat{d}(\ell_1, \ell_2) = d(\ell_1, \ell_2)$ otherwise; the following holds: $\text{SED}(\mathcal{G}_1, \mathcal{G}_2) = \widehat{\text{GED}}(\mathcal{G}_1, \mathcal{G}_2)$, where $\widehat{\text{GED}}$ denotes GED with \widehat{d} as the label set distance function. In simple words, the SED between two graphs is equivalent to GED with a label set distance function where we ignore insertion costs.*

PROOF. It suffices to prove (i) $\text{SED}(\mathcal{G}_1, \mathcal{G}_2) \geq \widehat{\text{GED}}(\mathcal{G}_1, \mathcal{G}_2)$ and (ii) $\widehat{\text{GED}}(\mathcal{G}_1, \mathcal{G}_2) \geq \text{SED}(\mathcal{G}_1, \mathcal{G}_2)$.

(i) Let $\mathcal{S} = (\mathcal{V}_{\mathcal{S}}, \mathcal{E}_{\mathcal{S}}, \mathcal{L}_{\mathcal{S}}) \subseteq \mathcal{G}_2$ be the subgraph minimizing $\text{SED}(\mathcal{G}_1, \mathcal{S})$ (Recall Eq. 3). Consider the mapping π from \mathcal{G}_1 to \mathcal{S} corresponding to $\text{SED}(\mathcal{G}_1, \mathcal{S})$ (and hence $\text{GED}(\mathcal{G}_1, \mathcal{S})$ as well). We extend π to define a mapping $\widehat{\pi}$ from \mathcal{G}_1 to \mathcal{G}_2 by mapping of all nodes in set $\mathcal{V}_2 \setminus \mathcal{V}_{\mathcal{S}}$ to dummy nodes in \mathcal{G}_1 ; the edge mappings are defined analogously.

Under this construction, $\text{SED}(\mathcal{G}_1, \mathcal{S}) = \text{GED}(\mathcal{G}_1, \mathcal{G}_2) = \widehat{\text{GED}}_{\widehat{\pi}}(\mathcal{G}_1, \mathcal{G}_2) \geq \widehat{\text{GED}}(\mathcal{G}_1, \mathcal{G}_2)$. This follows from the property that under \widehat{d} , insertion costs are zero, that is $\widehat{d}(\epsilon, \ell) = 0$. Thus, the additional mappings introduced in $\widehat{\pi}$ do not incur additional costs under \widehat{d} .

(ii) Consider $\mathcal{S} \subseteq \mathcal{G}_2$ and a mapping π from \mathcal{G}_1 to \mathcal{S} such that $\text{GED}_{\pi}(\mathcal{G}_1, \mathcal{S}) = \widehat{\text{GED}}(\mathcal{G}_1, \mathcal{G}_2)$. The existence of such a subgraph is guaranteed (See Lemma 5 in Supplementary). From the definition of GED, $\text{GED}_{\pi}(\mathcal{G}_1, \mathcal{S}) \geq \text{GED}(\mathcal{G}_1, \mathcal{S})$. Furthermore, since $\mathcal{S} \subseteq \mathcal{G}_2$, $\text{GED}(\mathcal{G}_1, \mathcal{S}) \geq \text{SED}(\mathcal{G}_1, \mathcal{G}_2)$. Combining all these results, we have $\widehat{\text{GED}}(\mathcal{G}_1, \mathcal{G}_2) \geq \text{GED}(\mathcal{G}_1, \mathcal{S}) \geq \text{SED}(\mathcal{G}_1, \mathcal{G}_2)$. Hence, the claim is proved. \square

Lemma 4 *\widehat{d} , as defined in Lemma 3, satisfies triangle inequality.*

PROOF. We need to show $\widehat{d}(\ell_1, \ell_3) \leq \widehat{d}(\ell_1, \ell_2) + \widehat{d}(\ell_2, \ell_3)$. We divide the proof into four cases:

- (i) None of ℓ_1, ℓ_2, ℓ_3 is ϵ . Hence, $\widehat{d}(\ell_1, \ell_3) = d(\ell_1, \ell_3)$ and triangle inequality is satisfied.
- (ii) $\ell_1 = \epsilon$. The LHS is 0 and hence triangle inequality is satisfied.
- (iii) $\ell_1 \neq \epsilon$ and $\ell_2 = \epsilon$. LHS ≤ 1 and RHS = 1. Hence, satisfied.
- (iv) Only $\ell_3 = \epsilon$. Here, LHS = 1 and RHS ≥ 1 .

These four cases cover all possible situations and hence, triangle inequality is established. \square

From Lemma 3, we know $\text{SED}(\mathcal{G}_1, \mathcal{G}_2) = \widehat{\text{GED}}(\mathcal{G}_1, \mathcal{G}_2)$. Combining Obs. 3 with Lemma 4, $\widehat{\text{GED}}$ satisfies triangle inequality. Thus, SED satisfies triangle inequality. \square

D.2 Proof of Lemma 5

Lemma 5 *There exists a subgraph \mathcal{S} of \mathcal{G}_2 and a node map π from \mathcal{G}_1 to \mathcal{S} such that $\text{GED}_{\pi}(\mathcal{G}_1, \mathcal{S}) = \widehat{\text{GED}}(\mathcal{G}_1, \mathcal{G}_2)$.*

PROOF. Let π' be a node map from \mathcal{G}_1 to \mathcal{G}_2 corresponding to $\widehat{\text{GED}}(\mathcal{G}_1, \mathcal{G}_2)$. Let h_1, \dots, h_l be the nodes of \mathcal{G}_2 which are inserted in π' . Construct subgraph \mathcal{S} of \mathcal{G}_2 by removing nodes h_1, \dots, h_l and their incident edges from \mathcal{G}_2 . Let π be the node map from \mathcal{G}_1 to \mathcal{S} which is obtained by removing h'_1, \dots, h'_l from the domain and h_1, \dots, h_l from the co-domain of π . Since insertion costs are 0 in \widehat{d} and π contains only non-insert operations, then $\text{GED}_{\pi}(\mathcal{G}_1, \mathcal{S}) = \widehat{\text{GED}}(\mathcal{G}_1, \mathcal{G}_2)$. Hence, the claim is proved. \square

Corollary 1 *There exists a closest subgraph (Def. 6) \mathcal{S} to \mathcal{G}_1 in \mathcal{G}_2 such that $\mathcal{S} \subseteq \mathcal{G}_1$.*

PROOF. The node map π in the above proof contains only non-insert operations. So, \mathcal{S} in the above proof is a subgraph of \mathcal{G}_1 ignoring node and edge labels. Since equality holds in Lemma 3, this π gives an optimal edit distance. Thus, \mathcal{S} in the above proof is also a closest subgraph to \mathcal{G}_1 in \mathcal{G}_2 . \square

D.3 More General Distance Functions

GED and SED can be viewed as error-tolerant graph and subgraph matching respectively. In practice, the edit costs are used to model the acceptable deviations from ideal graph patterns. The more tolerant we are towards a certain kind of distortion, the smaller is its corresponding edit cost. Concrete values for the edit costs are application-dependent. In this paper we have discussed binary distance functions which impose a cost of 1 for unequal labels and 0 for equal labels as these are the most popular distance functions used in literature. However our framework is also suitable for more general distance functions.

The results for GED directly extend to *any metric distance function* over the label set. The relevant proofs mentioned in the paper are directly applicable.

The results for SED can be extended to metric distance functions d over Σ for which replacement is no more expensive than deletion, i.e. $d(\ell_1, \ell_2) \leq d(\ell_1, \epsilon) \forall \ell_1, \ell_2 \in \Sigma$. A replacement can be seen as a compound edit operation consisting of deletion(s) followed by insertion(s). If a replacement cost is too high, replacement can be better achieved by deletion(s) followed by insertion(s), of which insertion(s) do not contribute to the cost in SED. Hence, this assumption is general enough to capture a large class of interesting distance functions which might be used for the SED prediction task. We show a generalisation of Lemma 4 to such distance functions d . The other proofs mentioned in the paper are directly applicable.

Lemma 6 *Let $d : \Sigma \times \Sigma \rightarrow \mathbb{R}_0^+$ be a metric and $d(\ell_1, \ell_2) \leq d(\ell_1, \epsilon) \forall \ell_1, \ell_2 \in \Sigma$. As in Lemma 3, let $\hat{d} : \Sigma \times \Sigma \rightarrow \mathbb{R}_0^+$ be a distance function over Σ , where (i) $\hat{d}(\ell_1, \ell_2) = 0$ if $\ell_1 = \epsilon$, and (ii) $\hat{d}(\ell_1, \ell_2) = d(\ell_1, \ell_2)$ otherwise. Then, \hat{d} satisfies the triangle inequality.*

PROOF. We need to show $\hat{d}(\ell_1, \ell_3) \leq \hat{d}(\ell_1, \ell_2) + \hat{d}(\ell_2, \ell_3)$. Consider the three cases:

- (i) $\ell_1 = \epsilon$. LHS = 0, RHS = $\hat{d}(\ell_2, \ell_3) \geq 0$ by non-negativity of d . Hence, LHS \leq RHS.
- (ii) $\ell_1 \neq \epsilon$ and $\ell_2 = \epsilon$. LHS = $d(\ell_1, \ell_2)$, RHS = $d(\ell_1, \epsilon)$. Hence, LHS \leq RHS by assumption.
- (iii) $\ell_1 \neq \epsilon$ and $\ell_2 \neq \epsilon$. LHS = $d(\ell_1, \ell_3)$, RHS = $d(\ell_1, \ell_2) + d(\ell_2, \ell_3)$. LHS \leq RHS by triangle inequality for d .

These cases cover all possible situations. Hence, triangle inequality is established. \square

D.4 Data Augmentation

Observation 4 *Let \mathcal{S} be a closest subgraph (Def. 6) of \mathcal{G}_1 in \mathcal{G}_2 . Let \mathcal{S}' be a subgraph of \mathcal{G}_2 which is also a supergraph of \mathcal{S} . Then \mathcal{S} is also a closest subgraph of \mathcal{G}_1 in \mathcal{S}' and $\text{SED}(\mathcal{G}_1, \mathcal{S}') = \text{SED}(\mathcal{G}_1, \mathcal{G}_2)$.*

PROOF. The set of subgraphs of \mathcal{S}' is a subset of the set of subgraphs of \mathcal{G}_2 . \mathcal{S} achieves the minimum $\text{GED}(\mathcal{G}_1, \mathcal{S})$ among all subgraphs of \mathcal{G}_2 and so also the minimum $\text{GED}(\mathcal{G}_1, \mathcal{S})$ among all subgraphs of \mathcal{S}' . Thus, $\text{SED}(\mathcal{G}_1, \mathcal{S}') = \text{SED}(\mathcal{G}_1, \mathcal{G}_2) = \text{GED}(\mathcal{G}_1, \mathcal{S})$. \square

Observation 4 gives a natural strategy for *data augmentation*. Once we have $\text{SED}(\mathcal{G}_1, \mathcal{G}_2)$ and a closest subgraph \mathcal{S} from the expensive non-neural computation of $\text{GED}(\mathcal{G}_1, \mathcal{G}_2)$, we can use $(\mathcal{G}_1, \mathcal{S}', \text{SED}(\mathcal{G}_1, \mathcal{G}_2))$ for all $\mathcal{S} \subseteq \mathcal{S}' \subseteq \mathcal{G}_2$ as training examples.

D.5 Triangle Inequality for \mathcal{F}

This is referred to in the proof for Lemma 1.

Lemma 7 $\mathcal{F}(\mathbf{Z}_{\mathcal{G}_Q}, \mathbf{Z}_{\mathcal{G}_T}) \leq \mathcal{F}(\mathbf{Z}_{\mathcal{G}_Q}, \mathbf{Z}_{\mathcal{G}_{T'}}) + \mathcal{F}(\mathbf{Z}_{\mathcal{G}_{T'}}, \mathbf{Z}_{\mathcal{G}_T})$, where $\mathcal{F}(\mathbf{x}, \mathbf{y}) = \|\text{ReLU}(\mathbf{x} - \mathbf{y})\|$ for any monotonic norm $\|\cdot\|$.

PROOF. Let $\mathbf{x}, \mathbf{y} \in \mathbb{R}^n$. We observe that $(\text{ReLU}(\mathbf{x}) + \text{ReLU}(\mathbf{y}))_i = \text{ReLU}(\mathbf{x})_i + \text{ReLU}(\mathbf{y})_i = \text{ReLU}(\mathbf{x}_i) + \text{ReLU}(\mathbf{y}_i) \geq \text{ReLU}(\mathbf{x}_i + \mathbf{y}_i) = (\text{ReLU}(\mathbf{x} + \mathbf{y}))_i$. Since $\|\cdot\|$ is monotonic, this implies $\|\text{ReLU}(\mathbf{x}) + \text{ReLU}(\mathbf{y})\| \geq \|\text{ReLU}(\mathbf{x} + \mathbf{y})\|$.

Using the triangle inequality for $\|\cdot\|$, we get $\|\text{ReLU}(\mathbf{x})\| + \|\text{ReLU}(\mathbf{y})\| \geq \|\text{ReLU}(\mathbf{x}) + \text{ReLU}(\mathbf{y})\| \geq \|\text{ReLU}(\mathbf{x} + \mathbf{y})\|$.

Substituting $\mathbf{x} = \mathbf{Z}_{\mathcal{G}_Q} - \mathbf{Z}_{\mathcal{G}_{T'}}$, $\mathbf{y} = \mathbf{Z}_{\mathcal{G}_{T'}} - \mathbf{Z}_{\mathcal{G}_T}$, we get, $\|\text{ReLU}(\mathbf{Z}_{\mathcal{G}_Q} - \mathbf{Z}_{\mathcal{G}_{T'}})\| + \|\text{ReLU}(\mathbf{Z}_{\mathcal{G}_{T'}} - \mathbf{Z}_{\mathcal{G}_T})\| \geq \|\text{ReLU}(\mathbf{Z}_{\mathcal{G}_Q} - \mathbf{Z}_{\mathcal{G}_T})\|$

This implies that $\mathcal{F}(\mathbf{Z}_{\mathcal{G}_Q}, \mathbf{Z}_{\mathcal{G}_{\mathcal{T}'}}) + \mathcal{F}(\mathbf{Z}_{\mathcal{G}_{\mathcal{T}'}}, \mathbf{Z}_{\mathcal{G}_{\mathcal{T}}}) \geq \mathcal{F}(\mathbf{Z}_{\mathcal{G}_Q}, \mathbf{Z}_{\mathcal{G}_{\mathcal{T}}})$. Our claim is proved. \square

E Computation Cost of SED and GED Inference

For this analysis, we make the simplifying assumption that the hidden dimension in the Pre-MLP, GIN and Post-MLP are all d . The average density of the graph is g . The number of hidden layers in Pre-MLP, and Post-MLP are L , and k in GIN.

The computation cost per node for each of these components are as follows.

- **Pre-MLP:** The operations in the MLP involve linear transformation over the input vector \mathbf{x}_v of dimension $|\Sigma|$, followed by non-linearity. This results in $O(|\mathcal{V}|(|\Sigma| \cdot d + d^2 L))$ cost.
- **GIN:** GIN aggregates information from each of the neighbors, which consumes $O(d \cdot g)$ time. The linear transformation consumes an additional $O(d^2)$ time. Applying non-linearity takes $O(d)$ time since it is a linear pass over the hidden dimensions. Finally these operations are repeated over each of the k hidden layers, results in a total $O(k(d^2 + dg))$ computation time per node. Across, all nodes, the total cost is $O(|\mathcal{V}|kd^2 + |\mathcal{E}|kd)$ time. The degree g terms gets absorbed since each edge passes message twice across all nodes.
- **Concatenation:** This step consumes $O(kd)$ time per node.
- **Pool:** Pool iterates over the GIN representation of each node requiring $O(|\mathcal{V}|dk)$ time.
- **Post-MLP:** The final MLP takes dk dimensional vector as input and maps it to a d dimensional vector over L layers. This consumes $O(kd^2 + d^2 L)$ time.

Combining all these factors, the total inference complexity for a graph is $O(|\mathcal{V}|(|\Sigma| \cdot d + d^2 L + kd^2) + |\mathcal{E}|kd)$. This operation is repeated on both the query and target graphs to compute their embeddings, on which distance function \mathcal{F} is operated. Thus, the final cost is $O(n(|\Sigma| \cdot d + d^2 L + kd^2) + m kd)$, where $n = |\mathcal{V}_Q| + |\mathcal{V}_{\mathcal{T}}|$ and $m = |\mathcal{E}_Q| + |\mathcal{E}_{\mathcal{T}}|$.

F Pipeline Details

Additional Model Details: We add residual connections [23] across blocks of two GIN convolution layers. This eases the flow of gradients to the earlier layers by skipping the intermediate non-linearities. We observed about 5x speedup in convergence and a marginal improvement in the generalisation error with residual connections. We use 8 layers, 64 hidden dimensions and 64 embedding dimensions. We use a single layer for pre-MLP and 2 layers with ReLU non-linearity for the other MLP’s.

Data generation: We generate training data under two different settings (described in § 4). SED computation is NP-hard, and to the best of our knowledge, there is no existing method which computes SED directly. Therefore, we generate the ground truth SED using existing methods on GED by leveraging Lemma 3 which establishes the relationship between SED and GED. More specifically, we use time limited *mixed integer programming* method MIP-F2 [32], which provides us with the best so far lower bound and upper bound for SED. The time limit is kept at 60 seconds per pair. Each pair is run with 64 threads on a 64 core machine. This gives sufficiently tight bounds (with exact values for a large majority of pairs). For evaluation, we use $\text{SED} = (\text{LB} + \text{UB})/2$ as the ground truth, where LB and UB are the lower and upper bounds respectively. Table 6 gives the tightness of SED bounds in the generated data.

| | Dblp | Amazon | PubMed | CiteSeer | Cora_ML | Protein | AIDS |
|-------------|-------|--------|--------|----------|---------|---------|-------|
| Range / SED | 0.434 | 0.409 | 0.039 | 0.188 | 0.103 | 0.202 | 0.004 |

Table 6: **Mean Relative Error in Generated Data. Here Range = UB – LB, and SED = (LB + UB)/2.**

Loss Function: While $\mathbf{Z}_{\mathcal{G}_Q}$ and $\mathbf{Z}_{\mathcal{G}_T}$ be the embeddings for the query graph \mathcal{G}_Q and target graph \mathcal{G}_T respectively, we use the following function (for training):

$$H(\mathbf{Z}_{\mathcal{G}_Q}, \mathbf{Z}_{\mathcal{G}_T}, l, u) = \begin{cases} (F(\mathbf{Z}_{\mathcal{G}_Q}, \mathbf{Z}_{\mathcal{G}_T}) - u)^2, & F(\mathbf{Z}_{\mathcal{G}_Q}, \mathbf{Z}_{\mathcal{G}_T}) > u \\ 0, & l \leq F(\mathbf{Z}_{\mathcal{G}_Q}, \mathbf{Z}_{\mathcal{G}_T}) \leq u \\ (l - F(\mathbf{Z}_{\mathcal{G}_Q}, \mathbf{Z}_{\mathcal{G}_T}))^2, & F(\mathbf{Z}_{\mathcal{G}_Q}, \mathbf{Z}_{\mathcal{G}_T}) < l \end{cases}$$

where l and u are the lower and upper bounds to SED in our generated data. With H , the parameters of the entire model are learned by minimizing the mean squared error.

$$\mathcal{L} = \frac{1}{|\mathbb{T}|} \sum_{\forall (\mathcal{G}_Q, \mathcal{G}_T, l, u) \in \mathbb{T}} H(\mathbf{Z}_{\mathcal{G}_Q}, \mathbf{Z}_{\mathcal{G}_T}, l, u) \quad (10)$$

Here, \mathbb{T} is the set of all training samples.

Training details: NEUROSED, NEUROSED-NN and NEUROSED-Dual were trained using the *AdamW* [36] optimizer with a weight decay of 10^{-3} . A batch-size of 200 graph pairs per mini-batch was used. The learning rate schedule was *cyclic* [45]. In each cycle, learning rate was increased from 0 to 10^{-3} for 2000 iterations and then decreased back to 0 for 2000 iterations. Training was stopped when the best validation loss did not improve for 5 cycles. We observe that a cyclic learning rate schedule usually gives faster and better convergence than the other attempted training schemes. A cyclic learning rate schedule allows using higher learning rates and thus speeds up training. It offers some regularisation due to the high learning rates seen in each cycle encouraging the optimizer to find flatter regions of minima, giving better generalisation. It is also robust to hyper-parameter settings.

Subgraph search via neighborhood decomposition:

For large target graphs, it is infeasible to compute the SED. In this paper, we proposed a *neighborhood decomposition* scheme to handle subgraph similarity queries in the following setting: compute the SED between the query and the k -hop neighborhood centered at each node in the target graph for some suitable k . The minimum SED thus computed can be considered as an approximation for the true SED. Ideally, such an SED would be an upper bound to the true SED. In our experiments the minimum SED is usually small. This is expected in general as the large targets graphs are likely to contain small query graphs (or their small variations). Thus the neighborhood decomposition is satisfactory for SED computation between small queries and large targets in practice. One practical advantage of using neighborhood decomposition is that it facilitates locating the region of the target graph where the closest subgraph is found. We rank these neighbourhoods and that allows us to consider regions of the target graph in order of relevance. This generates much smaller candidate sets and traditional expensive methods can be used to refine these candidate sets further.

In this section, we seek to give further insight into the efficacy of neighborhood decomposition and design guidelines for choosing the right value of k depending on the expected query distribution. In practice, we are concerned only with connected subgraphs. Assuming that all the closest subgraphs (Def. 6) are connected leads to the following result:

Theorem 3 *Assuming that all closest subgraphs are connected, a closest subgraph \mathcal{S} to \mathcal{G}_1 in \mathcal{G}_2 can be found in an $l/2$ -hop neighborhood \mathcal{N}_v , centered at some $v \in \mathcal{V}_{\mathcal{G}_2}$, where l is the length of the longest path in \mathcal{G}_1 .*

PROOF. By Corollary 1, there exists a closest subgraph \mathcal{S} of \mathcal{G}_1 in \mathcal{G}_2 which is also a subgraph of \mathcal{G}_1 ignoring node and edge labels. Under our assumption \mathcal{S} is connected. So, the diameter of \mathcal{S} is \leq the length l of the longest path in \mathcal{G}_1 . Since $\mathcal{S} \subseteq \mathcal{G}_2$, \mathcal{S} is contained in some $l/2$ neighborhood of \mathcal{G}_2 . \square

Finding the length of the longest path is NP-hard. However, we do not need to find the exact length of the longest path: any upper bound suffices. Moreover we do not even need the length of the longest path for l . The closest subgraph having a diameter equal to l is rare. In practice, the diameter of the closest subgraph is unlikely to be much higher than the diameter of the query itself.

In conclusion, subgraph similarity search suffers from the problem of an exponential search space of subgraphs. We resolve this issue in two ways: the neighborhood decomposition allows us to consider a number of subgraphs linear in the number of nodes in the target, all of which are much

smaller than the target graph itself. Second, our neural model learns to predict the SED directly with the small neighborhood sizes which make training data generation as well as neural processing using GNNs computationally feasible.

G Datasets

Dblp: Dblp is a co-authorship network where each node is an author and two authors are connected by an edge if they have co-authored a paper. The label of a node is the venue where the authors has published most frequently. The dataset has been obtained from <https://www.aminer.org/citation>. Considering the intractability of obtaining ground-truth SED for large graphs and many node labels, we only take nodes with neighborhood size ≤ 1000 , and group the node labels into 8 classes.

Amazon: Each node in Amazon represents a product and two nodes are connected by an edge if they are frequently co-purchased. The graph is unlabeled and hence equivalent to a graph containing a single label on all nodes. The dataset has been downloaded from [33].

PubMed: PubMed dataset is a citation network which consists of scientific publications from PubMed database pertaining to diabetes classified into one of three classes.

Protein: Protein dataset consists of protein graphs. Each node is labeled with a one of three functional roles of the protein.

AIDS: AIDS dataset consists of graphs constructed from the AIDS antiviral screen database. These graphs representing molecular compounds with Hydrogen atoms omitted. Atoms are represented as nodes and chemical bonds as edges.

CiteSeer: CiteSeer is a citation network which consists of scientific publications classified into one of six classes. Generally a smaller version is used for this dataset, but we use the larger version from [8].

Cora_ML: Cora dataset is a citation dataset consisting of many scientific publications classified into one of seven classes based on paper topic. Cora_ML is a smaller dataset extracted from Cora [8].

AIDS': AIDS' dataset is another collection of graphs constructed from the AIDS antiviral screen database. The graphs and their properties differ from those in AIDS. These graphs also represent chemical compound structures.

Linux: Linux dataset is a collection of program dependence graphs, where each graph is a function and nodes represent statements while edges represent dependency between statements.

IMDB: IMDB dataset is a collection of ego-networks of actors/actresses that have appeared together in any movie.

We use the same versions of AIDS', Linux, and IMDB as used in [2]. For all datasets, we use only connected graphs.

H Experimental Setup

Hardware Details: We use a machine with an Intel Xeon Gold 6142 processor and GeForce GTX 1080 Ti GPU for all our experiments.

Baselines: Here we describe the changes made to neural baselines to adapt to SED problem.

- SIMGNN [2] and H^2MN-NE/H^2MN-RW [53]: We train the model with $\frac{LB+UB}{2}$ as the ground truth value of SED (LB and UB are lower and upper bounds for SED respectively). Now let \mathcal{G}_1 be the query graph, and \mathcal{G}_2 be the target graph, we use $nSED(\mathcal{G}_1, \mathcal{G}_2) = \frac{SED(\mathcal{G}_1, \mathcal{G}_2)}{|\mathcal{G}_1|}$ instead of $nGED(\mathcal{G}_1, \mathcal{G}_2) = \frac{GED(\mathcal{G}_1, \mathcal{G}_2)}{(|\mathcal{G}_1|+|\mathcal{G}_2|)/2}$ as the normalized value of similarity in SIMGNN. This is because the absolute value of SED scales with the size of the query, as opposed to GED, which scales with size of the query as well as the target.
- NEUROMATCH [37]: We use the *un-anchored* version of NEUROMATCH trained on its original task (subgraph isomorphism decision problem) using its own training framework. For ranking, we use the violation scores it produces directly rather than thresholding the violation and predicting

| Methods | Dblp | Amazon | PubMed | CiteSeer | Cora_ML | Protein | AIDS | Methods | AIDS' | Linux | IMDB |
|----------------------|--------------|--------------|--------------|--------------|--------------|--------------|--------------|-----------------------|--------------|--------------|--------------|
| NEUROSED | 0.626 | 0.207 | 0.474 | 0.332 | 0.432 | 0.377 | 0.401 | NEUROSED _G | 0.629 | 0.318 | 3.612 |
| H ² MN-RW | 0.926 | 0.480 | 0.764 | 0.882 | 0.824 | 0.575 | 0.566 | H ² MN-RW | 0.777 | 0.534 | 28.486 |
| H ² MN-NE | 0.966 | 0.465 | 0.831 | 1.094 | 0.797 | 0.518 | 0.510 | H ² MN-NE | 0.779 | 0.176 | 28.182 |
| SIMGNN | 0.911 | 1.257 | 0.853 | 1.068 | 0.841 | 0.835 | 0.545 | SIMGNN | 0.816 | 0.489 | 28.082 |
| BRANCH | 2.156 | 3.697 | 1.692 | 2.275 | 2.277 | 1.986 | 1.092 | Branch | 2.895 | 2.017 | 3.303 |
| MIP-F2 | 2.165 | 3.303 | 1.528 | 1.940 | 1.834 | 1.264 | 0.684 | MIP-F2 | 2.184 | 0.480 | 36.460 |

(a) Prediction of SED.

(b) Prediction of GED

Table 7: MAE scores (lower is better) in (a) SED and (b) GED.

| Methods | Dblp | Amazon | PubMed | CiteSeer | Cora_ML | Protein | AIDS | Methods | AIDS' | Linux | IMDB |
|----------------------|-------------|-------------|-------------|-------------|-------------|-------------|-------------|-----------------------|------------|------------|------------|
| NEUROSED | 0.97 | 0.99 | 0.99 | 0.99 | 0.99 | 0.98 | 0.98 | NEUROSED _G | .91 | .97 | .99 |
| H ² MN-RW | 0.94 | 0.97 | 0.97 | 0.98 | 0.97 | 0.94 | 0.95 | H ² MN-RW | .86 | .92 | .66 |
| H ² MN-NE | 0.93 | 0.98 | 0.97 | 0.97 | 0.98 | 0.96 | 0.96 | H ² MN-NE | .86 | .98 | .65 |
| SIMGNN | 0.94 | 0.85 | 0.97 | 0.97 | 0.97 | 0.9 | 0.95 | SIMGNN | .84 | .93 | .80 |
| BRANCH | 0.75 | 0.63 | 0.88 | 0.91 | 0.86 | 0.64 | 0.82 | Branch | -.55 | .14 | .98 |
| MIP-F2 | 0.65 | 0.44 | 0.80 | 0.83 | 0.79 | 0.68 | 0.78 | MIP-F2 | -.20 | .78 | .69 |

(a) Prediction of SED.

(b) Prediction of GED

Table 8: R^2 scores (higher is better, 1 is maximum) in (a) SED and (b) GED.

subgraph isomorphism as intended. We change the size limits for sampling query/target graphs in training to better fit our data distribution.

Software details: We used PyTorch [39] and PyTorch-Geometric [20] for implementation. All experiments were done using Jupyter Notebooks [28]. The full code, notebooks for all experiments and the generated data are available at our GitHub repository⁴.

I Additional Results

I.1 Other measures for predicting SED and GED

In Section 4.2, we present the accuracy of all techniques on SED and GED in terms of *Root Mean Square Error (RMSE)*. Here we evaluate the same performance using several other metrics such as Mean Absolute Error (MAE) and R^2 . Tables 7a and 7b show the MAE scores for SED and GED respectively. Tables 8a and 8b present the results based on R^2 results. Consistent with the previous results, NEUROSED outperforms all techniques both in SED and GED in these two measures except BRANCH is competitive only on IMDB for GED prediction and H²MN-NE is better in Linux only for GED prediction.

I.2 Precision@k on k-NN queries

Fig. 7 shows Precision@k on k-NN queries. As visible, NEUROSED is comfortably among the best performing algorithms.

I.3 Additional Results on Ablation Study

Impact of GIN: To highlight the importance of GIN, we conduct ablation studies by replacing the GIN convolution layers in the model with several other convolution layers. As visible in the Table 9, GIN consistently achieves the best accuracy. This is not surprising since GIN is provably the most expressive among GNNs in distinguishing graph structures (essential to SED or GED computation) and is as powerful as the Weisfeiler-Lehman Graph Isomorphism test [49].

⁴<https://github.com/idea-iitd/NeuroSED>

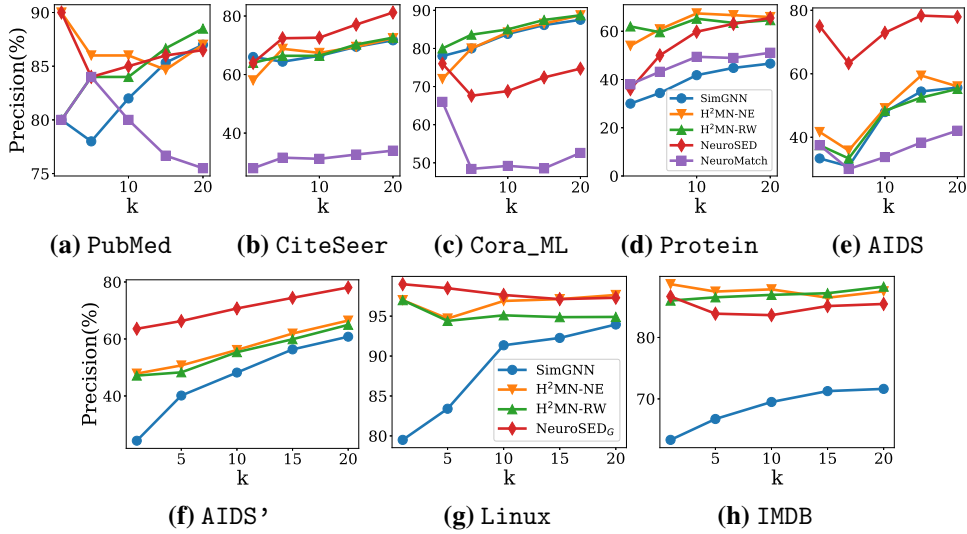


Figure 7: Precision@ k for k -NN queries on SED (a-e) and GED (f-h).

Impact of sum-pool: To substantiate our choice of the pooling layer, we have performed ablation studies with various pooling functions as replacements for sum-pool. It is clear from Table 10 that sum-pool is the best choice among the considered alternatives.

I.4 Alignment

In real-world applications of subgraph similarity search, alignments are of interest only for a small number of similar subgraphs. Our framework is intended to serve as a filter to retrieve this small set of similar subgraphs from a large number of candidates. To elaborate, a graph database may contain thousands or millions of graphs (or alternatively, thousands or millions of neighborhoods of a large graph) which need to be inspected for similar subgraphs. A user is typically interested in only a handful of these subgraphs that are highly similar to the query. Since the filtered set is significantly smaller, a non-neural exact algorithm suffices to construct the alignments (Lemma 3 allows us to adapt general cost GED alignment techniques for SED alignment). Computing alignments across the entire database is unnecessary and slows down the query response time.

To substantiate our claim, we show the average running time for answering 10-NN queries. We break up the running time into two components: (i) k -NN retrieval time by NEUROSED, (ii) exact alignment time using MIP-F2 for the 10-NN neighborhoods retrieved by NEUROSED. We observe that exact alignment by existing methods on the 10-NN neighborhoods completes in reasonable time. In contrast, GENN-A* does not scale on either PubMed or Amazon since it computes alignments across *all* (sub)graphs.

| Methods | Amazon (SED) | PubMed (SED) | CiteSeer (SED) | IMDB (GED) |
|---------------------------|--------------|--------------|----------------|--------------|
| NEUROSED (GIN) | 0.495 | 0.728 | 0.519 | 6.734 |
| NEUROSED-GCN | 0.532 | 0.756 | 0.556 | 12.151 |
| NEUROSED-GRAPHSAGE | 1.841 | 1.156 | 1.364 | 91.312 |
| NEUROSED-GAT | 1.843 | 1.259 | 1.294 | 89.034 |

Table 9: Ablation studies: GIN vs others. RMSE produced by different methods are shown and NEUROSED with GIN produces the best results.

| Pool functions | Amazon (SED) | PubMed (SED) | CiteSeer (SED) | IMDB (GED) |
|---------------------------|--------------|--------------|----------------|--------------|
| NEUROSED (Sum) | 0.495 | 0.728 | 0.519 | 6.734 |
| NEUROSED-Max | 0.603 | 0.709 | 0.795 | 52.519 |
| NEUROSED-Mean | 0.846 | 0.732 | 0.922 | 52.483 |
| NEUROSED-Attention | 0.868 | 0.797 | 0.914 | 130.47 |

Table 10: **Ablation studies: sum-pool vs others.** The sum-pool is the best choice among the considered alternatives.

| Methods | Amazon | PubMed |
|---------------------------|--------|--------|
| NEUROSED Retrieval | 6.471 | 0.373 |
| MIP-F2 Alignment | 68.4 | 52.8 |

Table 11: **The average runtime components in seconds for 10-NN query. MIP-F2 alignment is feasible for a small number of graphs retrieved by NEUROSED.**

J Retrieval using Index Structures

Linear Scan: For a new query G_Q , we first obtain its embedding \mathbf{Z}_{G_Q} . Based on the stored embeddings \mathbf{Z}_{G_T} of the target graphs, we compute $\text{SED}(\mathbf{Z}_{G_Q}, \mathbf{Z}_{G_T})$ for all $\mathbf{Z}_{G_T} \in \mathbf{Z}_{G_T}$ using the function $\mathcal{F}(\mathbf{Z}_{G_Q}, \mathbf{Z}_{G_T})$. We sort the targets based on the obtained SED values and use it to answer k -NN and range queries. Note that all target graphs are scanned for every query.

Adapted Metric Tree: Our adaptation of Metric Tree [46] to asymmetric functions satisfying triangle inequality is shown in Algorithms 1 and 2 (k -NN query is similar, see code for details). This speeds up retrieval by avoiding SED prediction for subtrees pruned using bounds derived from triangle inequality. A similar modification can be applied to more advanced index structures, such as M-Tree [13] which also supports efficient dynamic insertion and deletion of graphs from the database.

The tree construction times were 0.139s, 2.98s and 16.8s for PubMed, Amazon and Dblp respectively.

Algorithm 1 BUILD

Input: set D of objects, distance function $d(x, y)$ which satisfies triangle inequality

Output: root node of the constructed tree

```

if  $D = \phi$  then
    return NULL
end if
select arbitrary pivot  $p \in D$ 
 $m_1 \leftarrow \text{MEDIAN}(\{d(p, y) : y \in D - \{p\}\})$ 
 $m_2 \leftarrow \text{MEDIAN}(\{d(y, p) : y \in D - \{p\}\})$ 
 $D_1 \leftarrow \{y : d(p, y) \leq m_1, d(y, p) \leq m_2\}$ 
 $D_2 \leftarrow \{y : d(p, y) \leq m_1, d(y, p) > m_2\}$ 
 $D_3 \leftarrow \{y : d(p, y) > m_1, d(y, p) \leq m_2\}$ 
 $D_4 \leftarrow \{y : d(p, y) > m_1, d(y, p) > m_2\}$ 
for  $i = 1$  to  $4$  do
     $t_i \leftarrow \text{BUILD}(D_i, d)$ 
end for
return  $\text{NODE}(p, m_1, m_2, t_1, t_2, t_3, t_4)$ 

```

Theorem 4 *Correctness of the adaptation.*

PROOF. We show that any pruning does not affect the correctness of the returned answer set.

Algorithm 2 RANGEQUERY

Input: query object q , threshold r , root node t of (sub)tree
Output: $\{y | d(q, y) \leq r\}$

```
if  $t = \text{NULL}$  then
    return  $\phi$ 
end if
let  $t = \text{NODE}(p, m_1, m_2, t_1, t_2, t_3, t_4)$ 
if  $d(p, q) \leq m_1 - r$  then
    mark  $t_3$  and  $t_4$  for pruning
end if
if  $d(q, p) > m_2 + r$  then
    mark  $t_1$  and  $t_3$  for pruning
end if
if  $d(q, p) \leq r - m_1$  then
     $S \leftarrow$  all  $y$  in  $t_1$  and  $t_2$ 
    mark  $t_1$  and  $t_2$  for pruning
else
     $S \leftarrow \phi$ 
end if
for  $i = 1$  to  $4$  do
    if  $t_i$  is not marked for pruning then
         $S \leftarrow S \cup \text{RANGEQUERY}(q, r, t_i)$ 
    end if
end for
return  $S$ 
```

1. If $d(p, q) \leq m_1 - r$, then for any y in the solution set $\{y | d(q, y) \leq r\}$, we have $d(p, y) \leq m_1$ using $d(p, y) \leq d(p, q) + d(q, y)$. Since t_3 and t_4 contain only y such that $d(p, y) > 1$, pruning them preserves the solution set.
2. If $d(q, p) > m_2 + r$, then for any y in the solution set $\{y | d(q, y) \leq r\}$, we have $d(y, p) > m_2$ using $d(q, p) \leq d(q, y) + d(y, p)$. Since t_1 and t_3 contain only y such that $d(y, p) \leq m_2$, pruning them preserves the solution set.
3. If $d(q, p) \leq r - m_1$, then for all y such that $d(p, y) \leq m_1$ we have $d(q, y) \leq r$ using $d(q, y) \leq d(q, p) + d(p, y)$. Since $d(p, y) \leq m_1$ for all y in the subtrees t_1 and t_2 , all y 's in t_1 and t_2 are parts of the solution set.

□

K Heat Maps for Prediction Error

In Figures 8 to 17, we show the variation of the errors on SED and GED prediction with query sizes and ground truth values for NEUROSED (NEUROSED G for GED) and the baselines on all the corresponding datasets. This experiment is an extension of the heat-map results in Fig. 3 in the main paper. These datasets show variations in the distributions of SED and GED values. It is interesting to observe that among the baselines, different methods perform well on different regions (e.g., combinations of high/low SED and high/low query sizes). In the figures, darker means higher error. The baselines do not show good performance on all regions. However, for NEUROSED and NEUROSED G , we see a much better coverage for all types of regions in the domain. Furthermore, for every region, our models outperform (or are at least competitive with) the best performing baseline for that region.

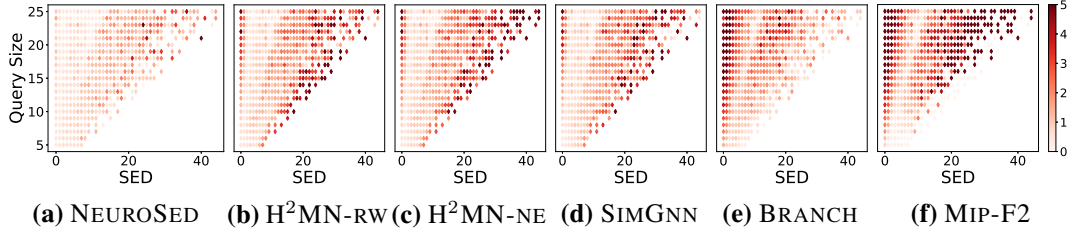


Figure 8: **Heat Maps of SED error against query size and SED values for DbLP.** Darker means higher error.

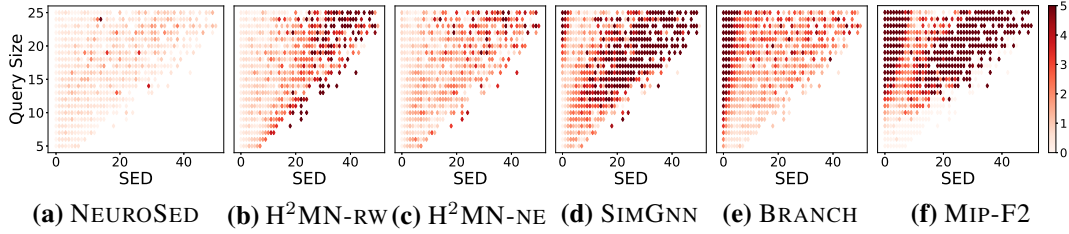


Figure 9: **Heat Maps of SED error against query size and SED values for Amazon.** Darker means higher error.

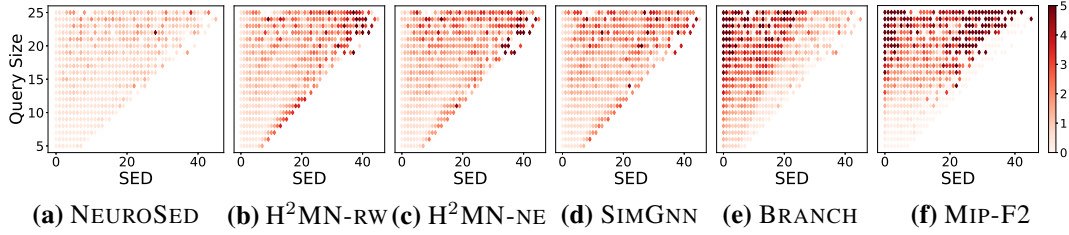


Figure 10: **Heat Maps of SED error against query size and SED values for PubMed.** Darker means higher error.

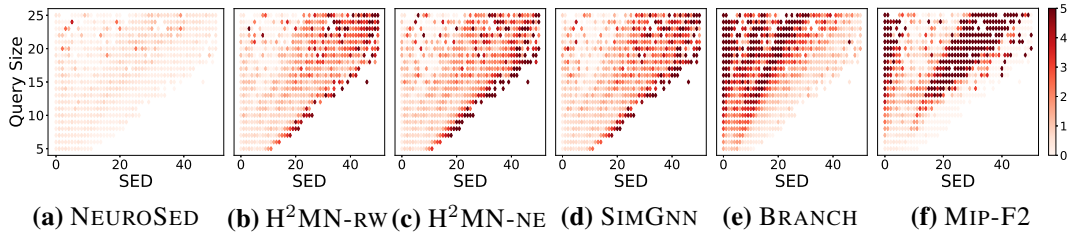


Figure 11: **Heat Maps of SED error against query size and SED values for CiteSeer.** Darker means higher error.

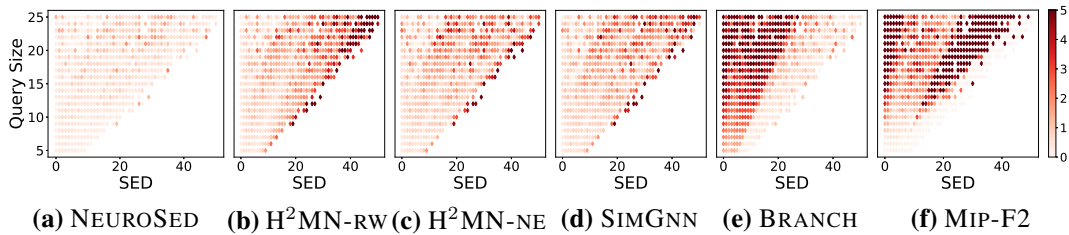


Figure 12: **Heat Maps of SED error against query size and SED values for Cora_ML.** Darker means higher error.

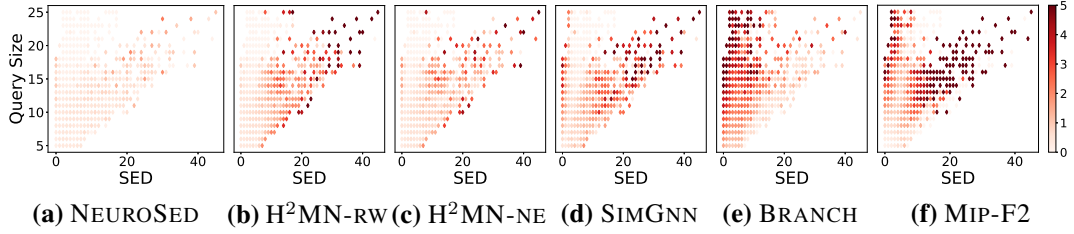


Figure 13: **Heat Maps of SED error against query size and SED values for Protein.** Darker means higher error.

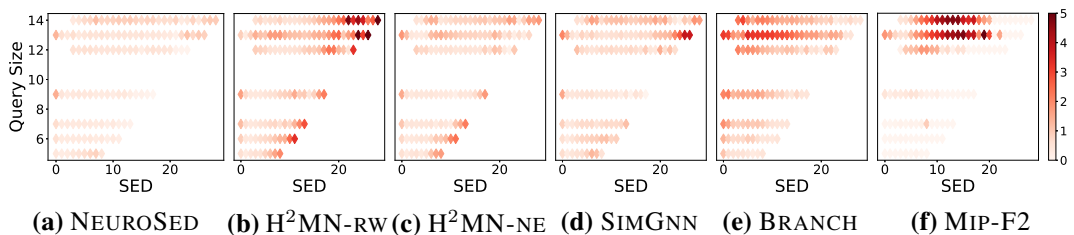


Figure 14: **Heat Maps of SED error against query size and SED values for AIDS.** Darker means higher error.

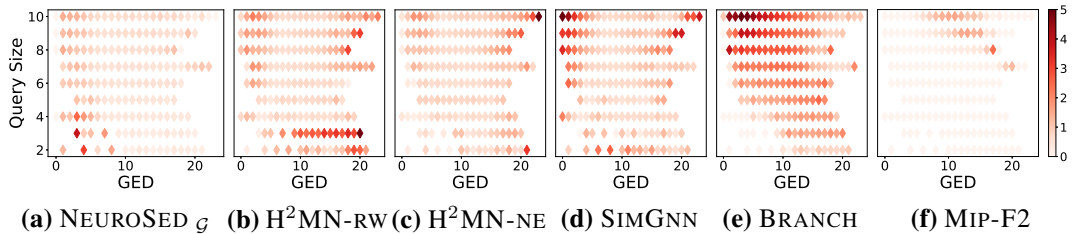


Figure 15: **Heat Maps of GED error against query size and GED values for AIDS'.** Darker means higher error.

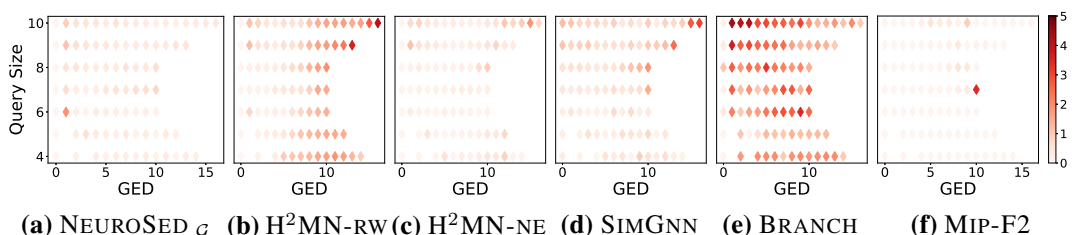


Figure 16: **Heat Maps of GED error against query size and GED values for Linux.** Darker means higher error.

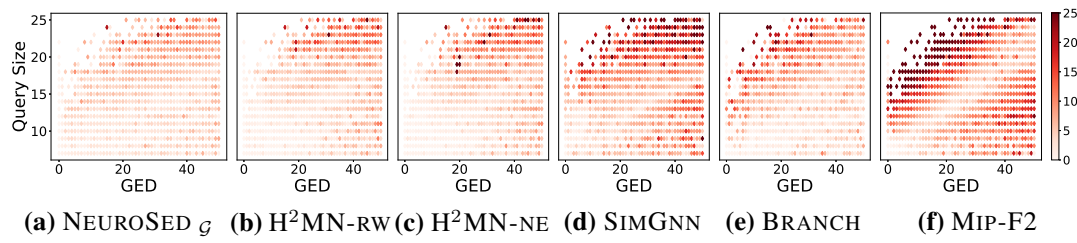


Figure 17: **Heat Maps of GED error against query size and GED values for IMDB. Darker means higher error.**